KTH Engineering Sciences

Calorimetry

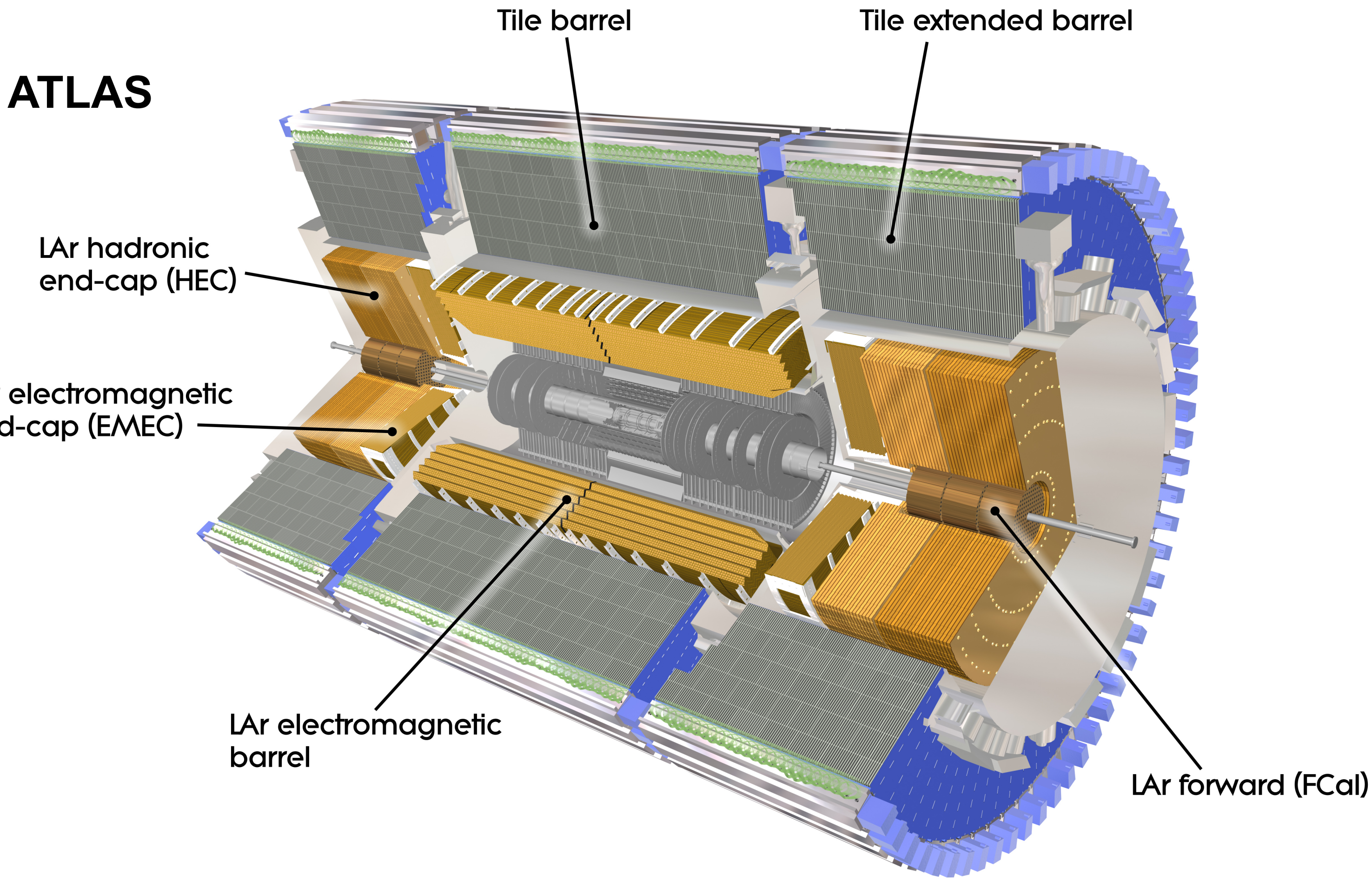

Lectures

To start:

- Introduction
- Detection mechanisms
- Review of particle interaction with matter
- Electromagnetic cascades

The further sections will include:

- Hadronic cascades
- Resolution
- Signal treatment and calibration
- Clustering, jets
- Hadronic compensation
- Examples of (expected) performances
- Jet substructure
- Particle flow

Introduction

KTH Engineering Sciences

Calorimetry

From Wikipedia

Calorimetry is the science of measuring the heat of chemical reactions or physical changes. Calorimetry involves the use of a calorimeter. The word calorimetry is derived from the Latin word *calor*, meaning heat. Scottish physician and scientist Joseph Black, who was the first to recognize the distinction between heat and temperature, is said to be the founder of calorimetry.[1]

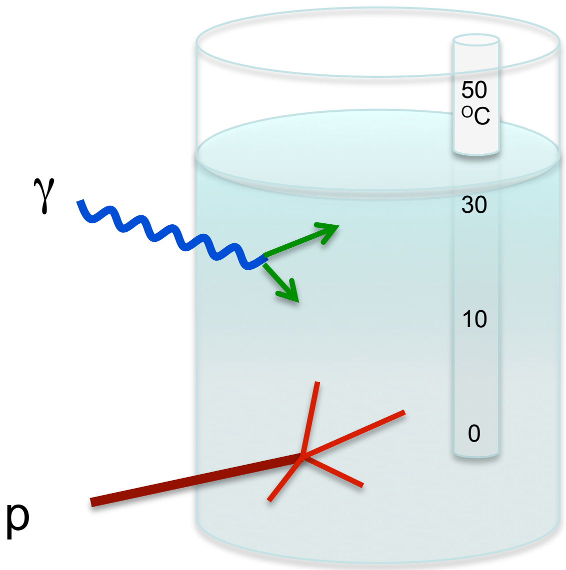

$$\Delta T = \frac{Q}{C}$$

The energy required to heat 1L of water 1K = 1 kCal = 2.611×10^{22} eV = 2.611×10^{10} TeV

Calorimetry in nuclear and particle physics:

- Measure the energy and properties of a particles by total absorption of their energy in a block of matter.
- Through a detection mechanism (scintillation light or ionization) a signal proportional to the energy of the incoming particle is obtained.
- The process is *destructive.*

- With the invention of the photomultiplier tube (PMT) the fluorescence in certain materials could be used to give quantitative measurements of particle properties in nuclear decays.

- Today we use calorimeters in a wide variety of experiments with varying resolutions.

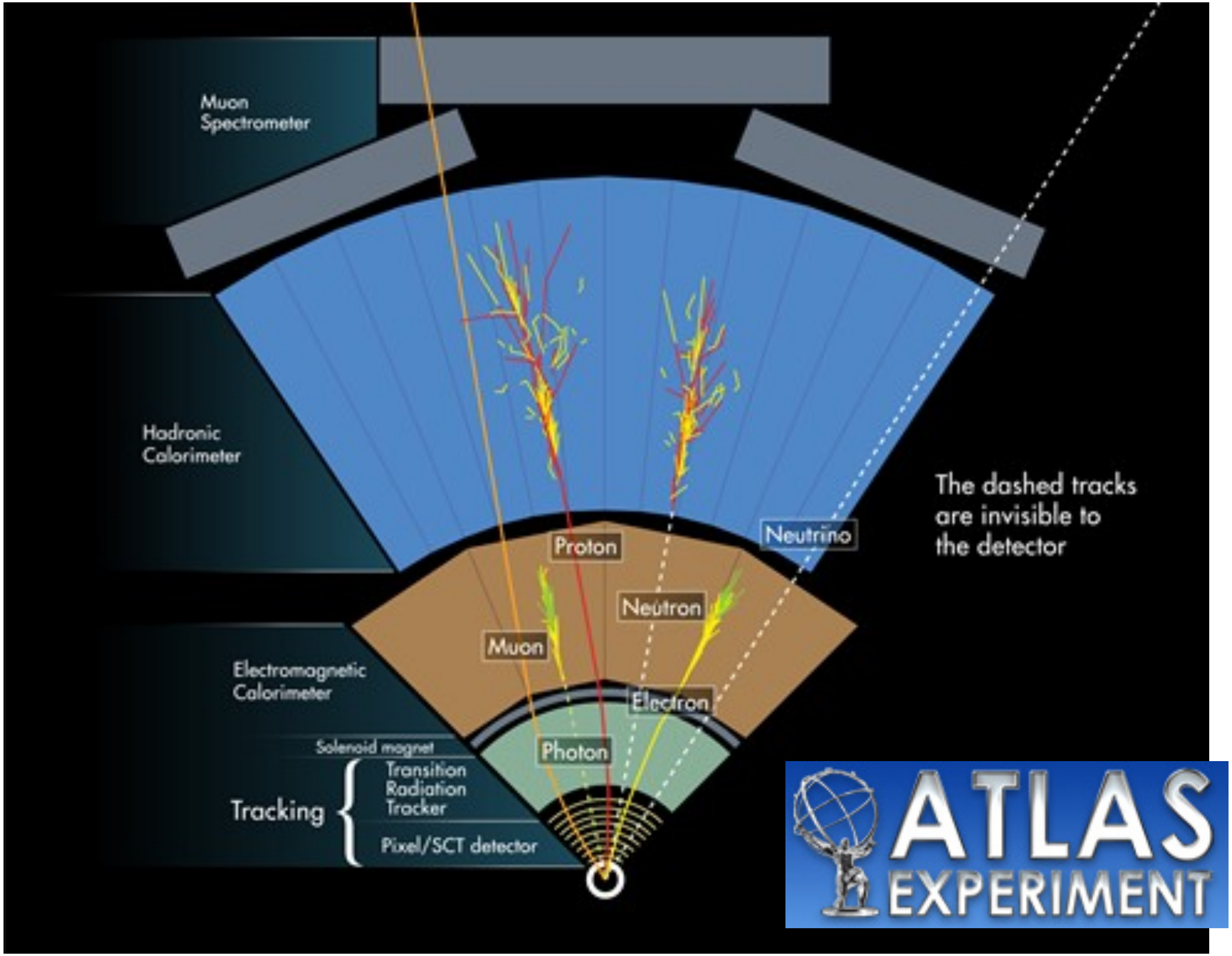

Muon Spectrometer
Hadronic Calorimeter
Electromagnetic Calorimeter
Solenoid magnet
Tracking
Transition Radiation Tracker
Pixel/SCT detector
Proton
Neutron
Muon
Electron
Photon
Neutrino
The dashed tracks are invisible to the detector
ATLAS EXPERIMENT

KTH Engineering Sciences

The choice of technique depends on requirements on e.g.

- energy resolution
- energy range
- position resolution
- timing
- radiation environment
- volume
- cost

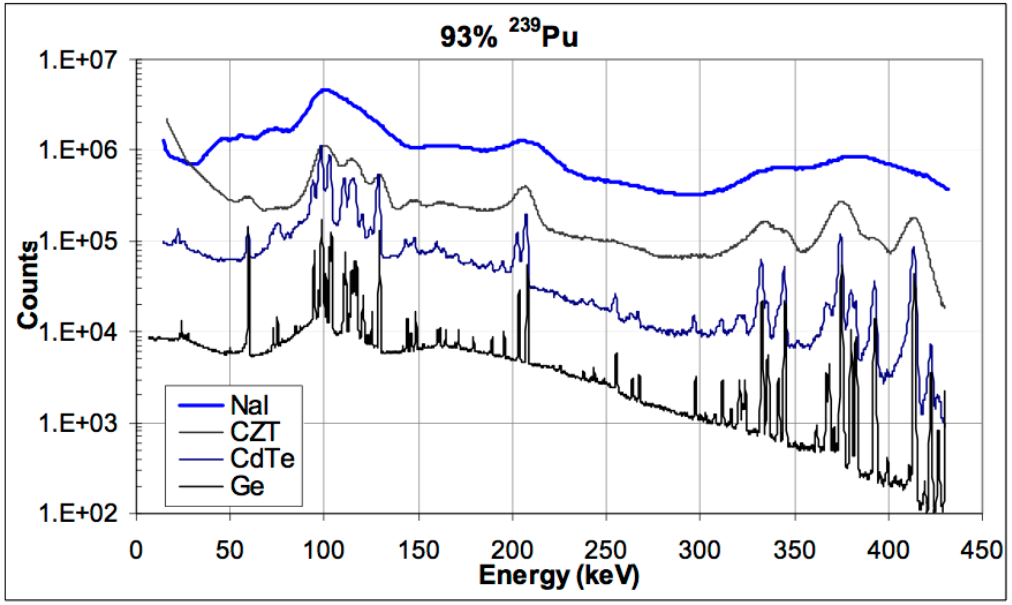

Fig. 1. Gamma-ray spectra of low-burnup (93% ^{239}Pu) plutonium measured with four different gamma-ray detectors: NaI:Tl, CPG CdZnTe, CdTe, and Ge (top to bottom). Refer to Table 1 for specifications on the detectors.

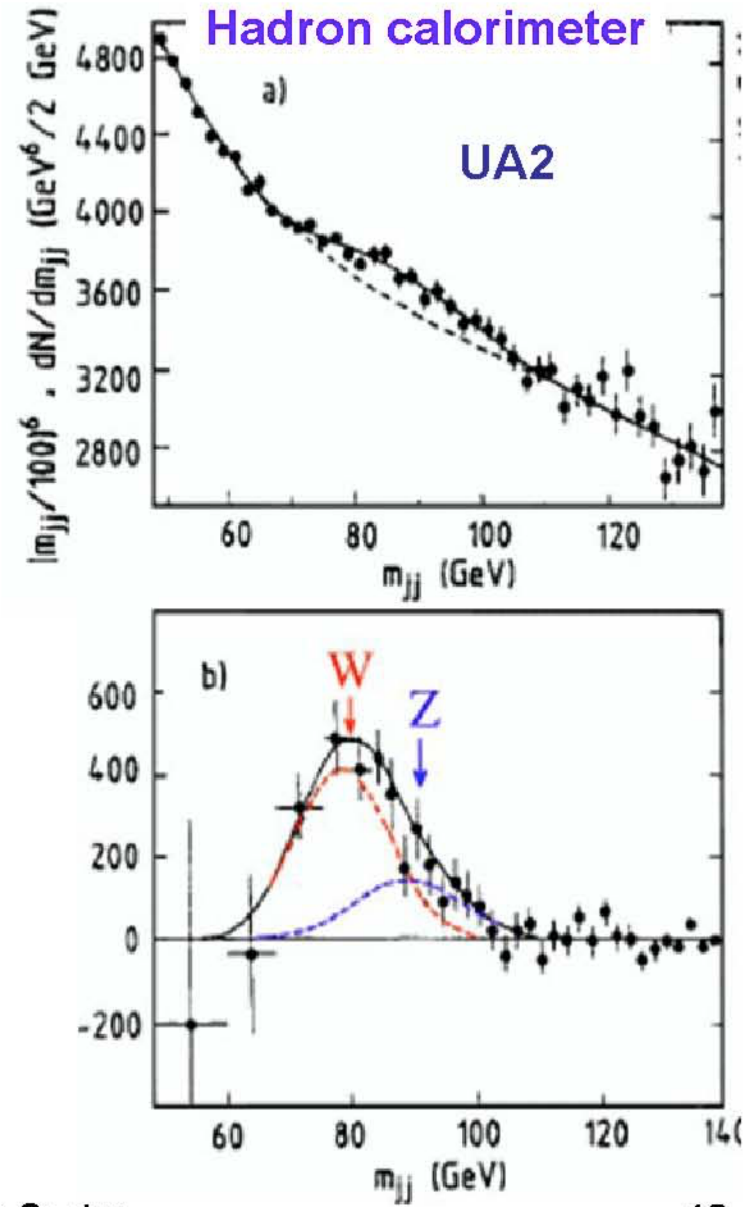

KTH Engineering Sciences

Detection mechanisms

Measuring particle properties, i.e. how the particle loses its energy in the block of matter, requires some sort of detection mechanism.

- Scintillation light
- Ionization
- Cherenkov radiation
- Cryogenic phenomena

The ”detection mechanism” introduces limitations and affects the design of the ”block of matter”.

Some limitations and design aspect will be discussed later.

KTH Engineering Sciences

Detection mechanisms: scintillation light

Traversing charged particles may bring atoms or molecules in an excited state.

The excited state is unstable (or metastable) and usually returns to its ground state by emitting one or more photons.

Visible photons: fluorescence or scintillation.

Deexcitation timescale: typically 10^{-12} to 10^{-6} s

Issues:

- deexcitation time
- wavelength
- light collection
- stability in time (aging)
- radiation hardness
- other possible environmental aspects like humidity

KTH Engineering Sciences

Detection mechanisms: ionisation

Traversing charged particles may ionise atoms during its passages.
The inonisation electrons are subsequently collected.

Liquid media: often enough ionisation electrons. No amplification used.
Example: LAr, LKr.
Gaseous media: use avalanche multiplication, e.g wirechamber or driftchamber types
Semiconductor detectors.

Issues:

- electron collection efficiency (usually requires high purity media with low oxygen contamination
- charge collection time

Detection mechanisms: cherenkov light

Charged particles traversing a medium with a velocity $v > c/n$ where n is the refractive medium emits chrenkov light.

The emission angle is given by $\cos \Theta_c = 1/(\beta n)$.

Instantaneous.

$1/\lambda^2$ spectrum $\Rightarrow$ blue light.

Issues:

- light collection
- angular dependence

Detection mechanisms: cryogenic phenomena

Specialised devices for dark matter searches, magnetic monoploes etc still under development operating in the sub-Kelvin range.

Some device types:

- Bolometers
- Superconducting tunnel junctions
- Superheated superconducting granules.

Review of particle interactions with matter

"Stopping power" (Bethe-Bloch)

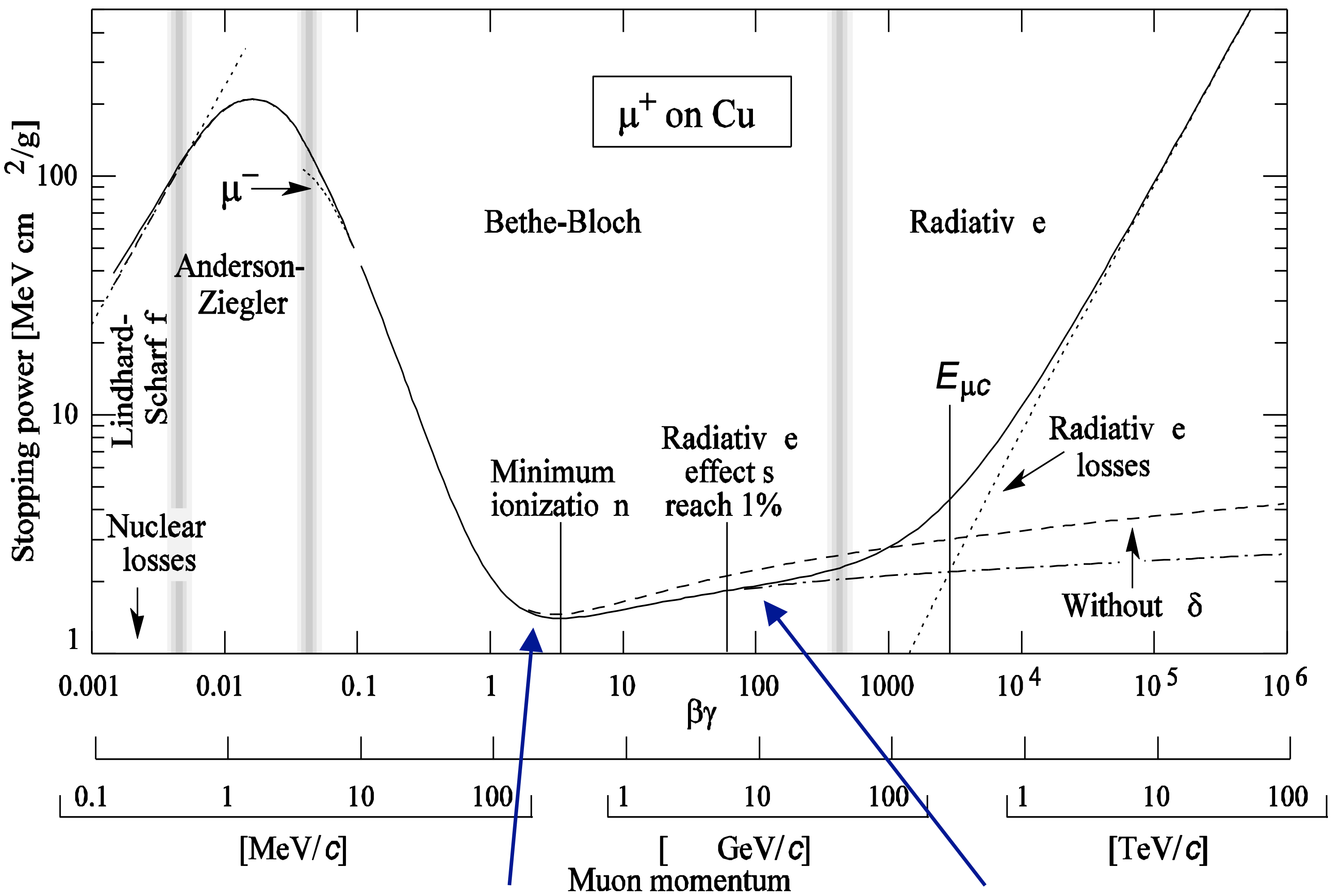

e+ and e- : modified B-B due to scattering and indist-inguish-ability of e-

Minimum at βγ ≈4

Logarithmic rise due to ln γ^2

Bremsstrahlung

e^+ and e^- : Radiation of real photons in the Coulomb field of the nuclei of the traversed medium

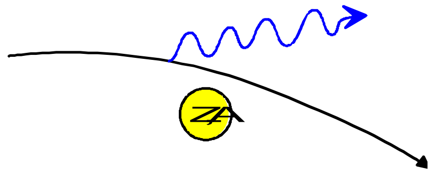

$$-\frac{dE}{dx} = 4\alpha \frac{N_A}{A} z^2 \left(\frac{1}{4\pi\varepsilon_0} \frac{e^2}{mc^2} \right)^2 E\{\ldots\} \propto \frac{E}{m^2}$$

e^-:

$$-\frac{dE}{dx} = 4\alpha N_A \frac{Z^2}{A} r_e{}^2 E \left\{ Z^2 \left[L_{rad} - f(Z) \right] + Z L'_{rad} \right\}$$

(Tsai, Rev. Mod. Phys 46 (1974) 38)

where $L_{rad} = \ln \frac{184.15}{Z^{1/3}}, \quad L'_{rad} = \ln \frac{1194}{Z^{2/3}}$ and

$$f(Z) \approx 1.202(\alpha Z)^2 - 1.0369(\alpha Z)^4 + 1.008 \frac{(\alpha Z)^6}{1 + (\alpha Z)^2}$$

Rewrite as: $-\frac{dE}{dx} = \frac{E}{X_0}$

Energy remaining for an e^- after distance x $\quad E = E_0 \, e^{-x/X_0}$

X_0 ≡ radiation length [g/cm^2]

An electron loses all but 1/e to bremsstrahlung over one X_0

Bremsstrahlung (2)

KTH Engineering Sciences

From PDG:

$$X_0 = \frac{716.4\,\mathrm{g\,cm^{-2}}\,A}{Z(Z+1)\ln(287/\sqrt{Z})}$$

$1X_0$ =

Al: 8.9 cm
Fe: 1.76 cm
Pb: 0.56 cm
W: 0.35 cm
Si: 8.9 cm
LN_2: 47.1 cm
LAr: 14.0 cm
LXe: 2.87 cm

6. Atomic and nuclear properties of materials 1

6. ATOMIC AND NUCLEAR PROPERTIES OF MATERIALS

Table 6.1 Abridged from pdg.lbl.gov/AtomicNuclearProperties by D. E. Groom (2007). See web pages for more detail about entries in this table including chemical formulae, and for several hundred other entries. Quantities in parentheses are for NTP (20° C and 1 atm), and square brackets indicate quantities evaluated at STP. Boiling points are at 1 atm. Refractive indices n are evaluated at the sodium D line blend (589.2 nm); values $\gg 1$ in brackets are for $(n-1)\times 10^6$ (gases).

Material	Z	A	$\langle Z/A \rangle$	Nucl.coll. length λ_T {g cm^{-2}}	Nucl.inter. length λ_I {g cm^{-2}}	Rad.len. X_0 {g cm^{-2}}	$dE/dx\|_{min}$ { MeV g^{-1}cm^2}	Density {g cm^{-3}} ({gℓ^{-1}})	Melting point (K)	Boiling point (K)	Refract. index (@ Na D)
H_2	1	1.00794(7)	0.99212	42.8	52.0	63.04	(4.103)	0.071(0.084)	13.81	20.28	1.11[132.]
D_2	1	2.01410177803(8)	0.49650	51.3	71.8	125.97	(2.053)	0.169(0.168)	18.7	23.65	1.11[138.]
He	2	4.002602(2)	0.49967	51.8	71.0	94.32	(1.937)	0.125(0.166)		4.220	1.02[35.0]
Li	3	6.941(2)	0.43221	52.2	71.3	82.78	1.639	0.534	453.6	1615.	
Be	4	9.012182(3)	0.44384	55.3	77.8	65.19	1.595	1.848	1560.	2744.	
C diamond	6	12.0107(8)	0.49955	59.2	85.8	42.70	1.725	3.520			2.42
C graphite	6	12.0107(8)	0.49955	59.2	85.8	42.70	1.742	2.210			
N_2	7	14.0067(2)	0.49976	61.1	89.7	37.99	(1.825)	0.807(1.165)	63.15	77.29	1.20[298.]
O_2	8	15.9994(3)	0.50002	61.3	90.2	34.24	(1.801)	1.141(1.332)	54.36	90.20	1.22[271.]
F_2	9	18.9984032(5)	0.47372	65.0	97.4	32.93	(1.676)	1.507(1.580)	53.53	85.03	[195.]
Ne	10	20.1797(6)	0.49555	65.7	99.0	28.93	(1.724)	1.204(0.839)	24.56	27.07	1.09[67.1]
Al	13	26.9815386(8)	0.48181	69.7	107.2	24.01	1.615	2.699	933.5	2792.	
Si	14	28.0855(3)	0.49848	70.2	108.4	21.82	1.664	2.329	1687.	3538.	3.95
Cl_2	17	35.453(2)	0.47951	73.8	115.7	19.28	(1.630)	1.574(2.980)	171.6	239.1	[773.]
Ar	18	39.948(1)	0.45059	75.7	119.7	19.55	(1.519)	1.396(1.662)	83.81	87.26	1.23[281.]
Ti	22	47.867(1)	0.45961	78.8	126.2	16.16	1.477	4.540	1941.	3560.	
Fe	26	55.845(2)	0.46557	81.7	132.1	13.84	1.451	7.874	1811.	3134.	
Cu	29	63.546(3)	0.45636	84.2	137.3	12.86	1.403	8.960	1358.	2835.	
Ge	32	72.64(1)	0.44053	86.9	143.0	12.25	1.370	5.323	1211.	3106.	
Sn	50	118.710(7)	0.42119	98.2	166.7	8.82	1.263	7.310	505.1	2875.	
Xe	54	131.293(6)	0.41129	100.8	172.1	8.48	(1.255)	2.953(5.483)	161.4	165.1	1.39[701.]
W	74	183.84(1)	0.40252	110.4	191.9	6.76	1.145	19.300	3695.	5828.	
Pt	78	195.084(9)	0.39983	112.2	195.7	6.54	1.128	21.450	2042.	4098.	
Au	79	196.966569(4)	0.40108	112.5	196.3	6.46	1.134	19.320	1337.	3129.	
Pb	82	207.2(1)	0.39575	114.1	199.6	6.37	1.122	11.350	600.6	2022.	
U	92	[238.02891(3)]	0.38651	118.6	209.0	6.00	1.081	18.950	1408.	4404.	
Air (dry, 1 atm)			0.49919	61.3	90.1	36.62	(1.815)	(1.205)		78.80	
Shielding concrete			0.50274	65.1	97.5	26.57	1.711	2.300			
Borosilicate glass (Pyrex)			0.49707	64.6	96.5	28.17	1.696	2.230			
Lead glass			0.42101	95.9	158.0	7.87	1.255	6.220			
Standard rock			0.50000	66.8	101.3	26.54	1.688	2.650			
Methane (CH_4)			0.62334	54.0	73.8	46.47	(2.417)	(0.667)	90.68	111.7	[444.]

Radiation length for a mixture of materials:

$$\frac{1}{X_0} = \sum_i V_i / X_i$$

where V_i is the volume fraction and X_i the radiation length

Similar for a compound material:

$$\frac{1}{X_0} = \sum_i m_i / X_i$$

where m_i is the mass fraction (and X_i is in g/cm^{2})

Critical energy

KTH Engineering Sciences

$$\left.\frac{dE}{dx}(E_c)\right|_{Brems} = \left.\frac{dE}{dx}(E_c)\right|_{ion}$$

(Definition)

For electrons one finds approximately:

$$E_c^{solid+liq} = \frac{610MeV}{Z+1.24} \qquad E_c^{gas} = \frac{710MeV}{Z+0.92}$$

density effect of dE/dx(ionisation) !

$E_c(e^-)$ in Fe(Z=26) = 22.4 MeV

For muons

$$E_c \approx E_c^{elec}\left(\frac{m_\mu}{m_e}\right)^2$$

$E_c(\mu)$ in Fe(Z=26) $\approx$ 1 TeV

E_c for some materials in MeV:

Pb	9.51
Fe	27.4
Air (NTP)	102
NaI	17.4
H_2O	92

KTH Engineering Sciences

Critical energy (2)

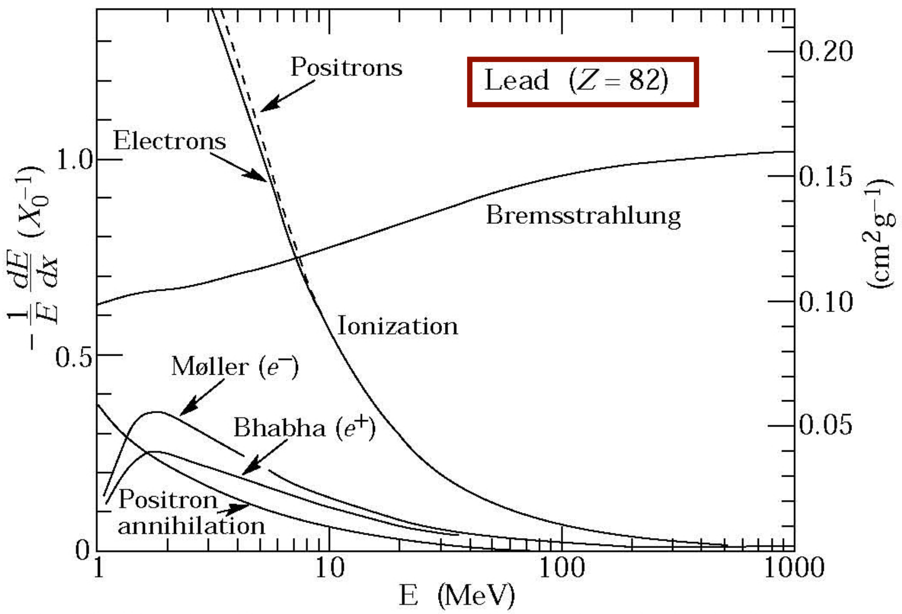

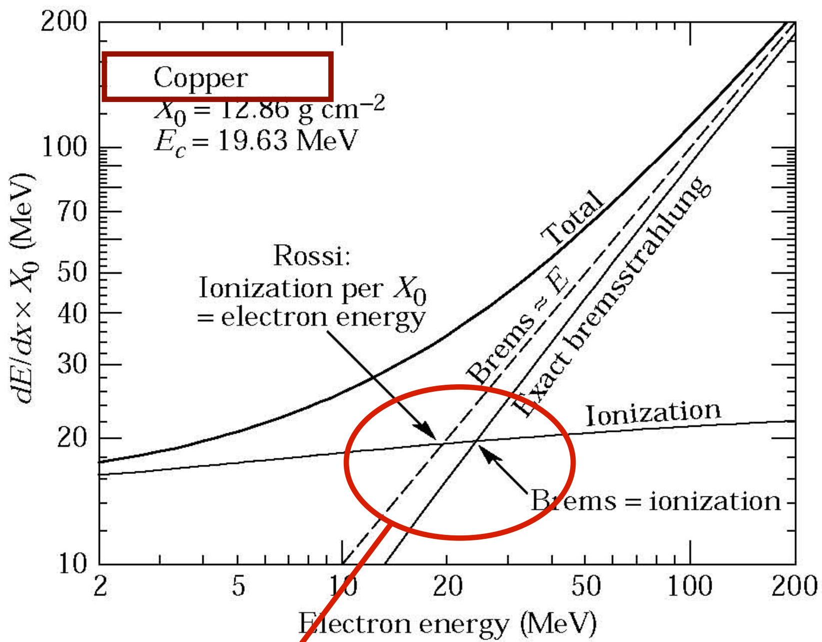

Critical energy :
Energy losses due to bremsstrahlung and ionisation are equal

Photon interactions with matter

Photoelectric effect

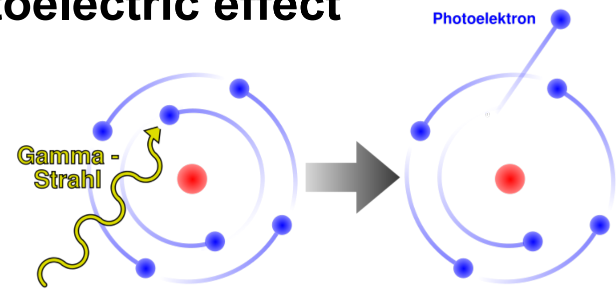

Compton scattering

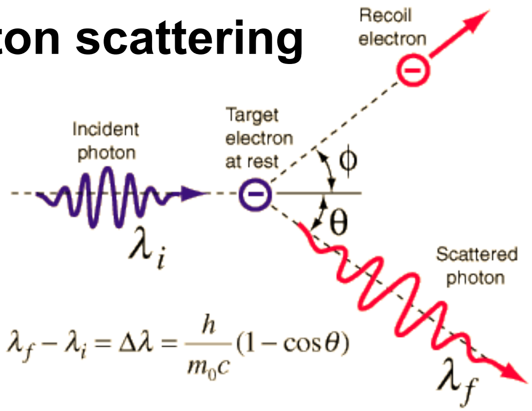

$$\lambda_f - \lambda_i = \Delta\lambda = \frac{h}{m_0 c}(1-\cos\theta)$$

Pair production

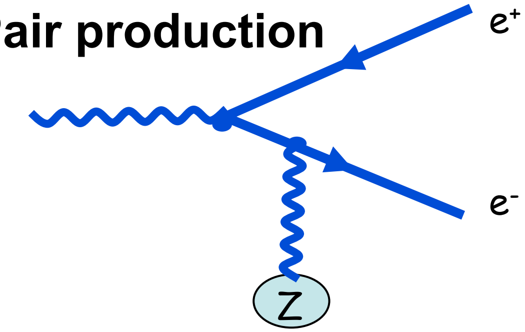

$$\sigma_{pair} \approx \frac{A}{N_A}\frac{7}{9}\frac{1}{X_0}$$

Mean free path for pair production: $9/7\ X_0$

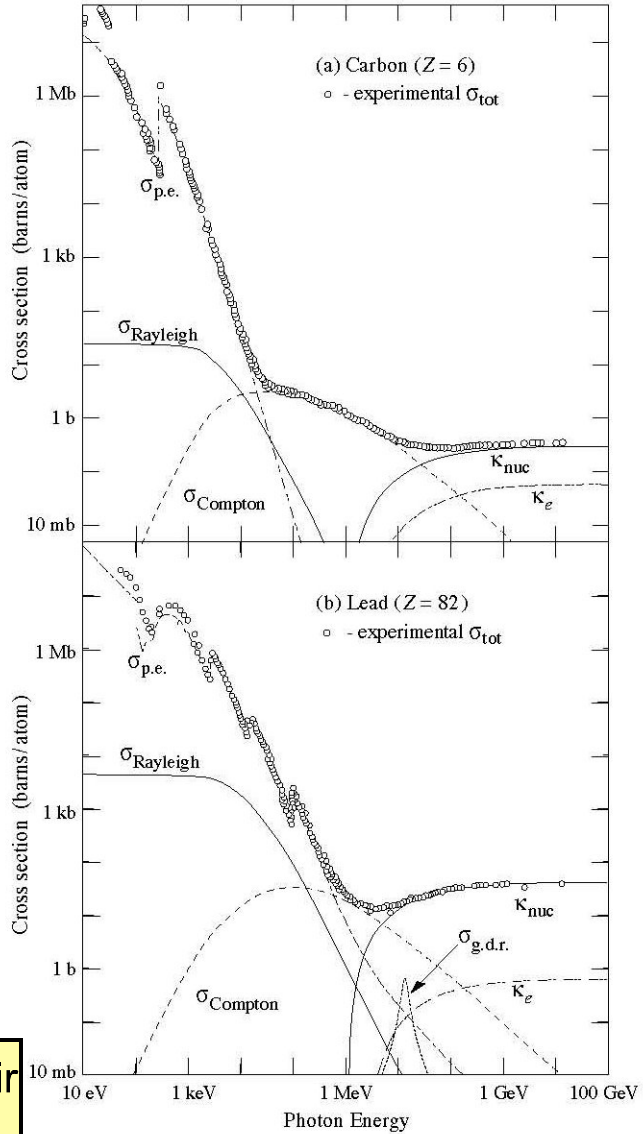

Electromagnetic Cascade

Very simplified model:

- e/γ with E> 1GeV mainly give secondary particlers in intercations (brems + pairprod.)
  - $E_i > E_c$: new e^+e^- pairs and γ are created but att lower and lower energy
  - $E_i < E_c$: the energy is absorbed (over a short distance) by ionisation processes

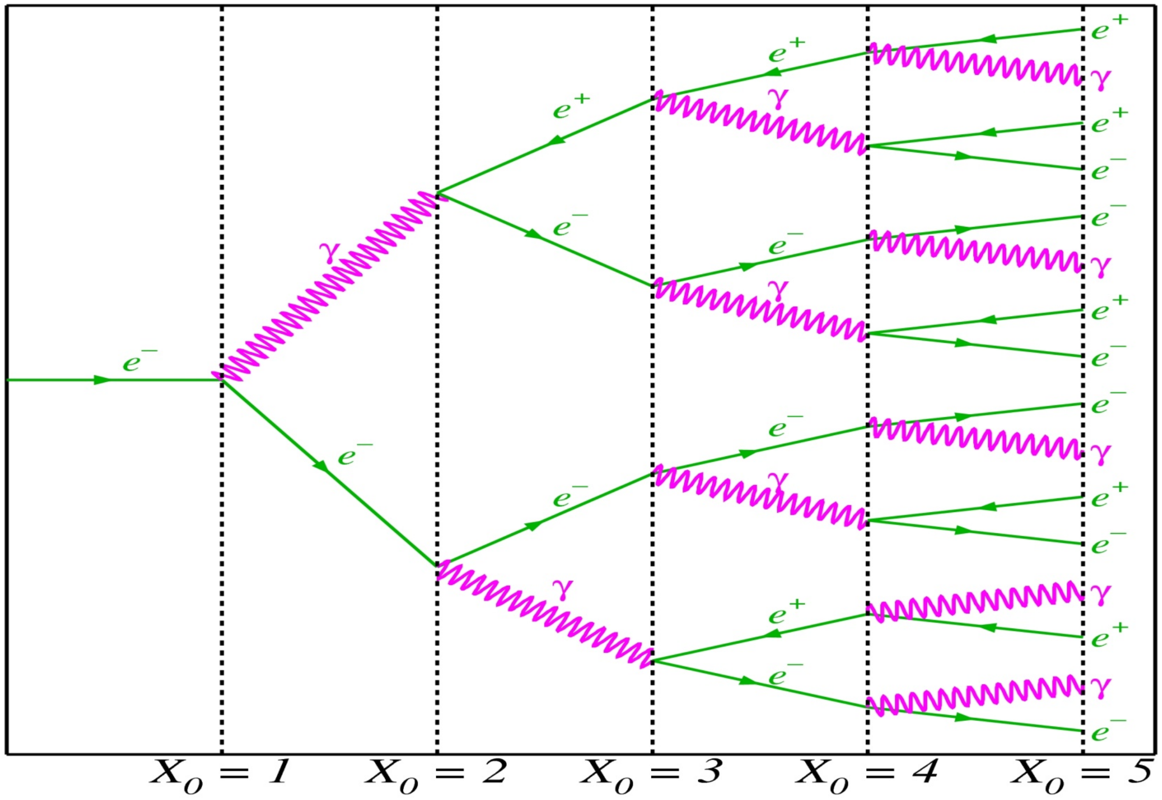

After nX_0 the total number of e and γ is $N(n)=2^n$.
Average particle energy: $E_0/2_n$

When $E(_n) = E_c$ the shower development stops!!!!

Shower length:
$n_{max}=1/\ln 2 \ \ln(E_0/E_c)$

Increases with ln E_0

Total number of electrons produced:

$$N^{total} = \sum_{n=0}^{n_{max}} 2^n = 2^{(n_{max}+1)} - 1 \approx$$

$$2 \cdot 2^{n_{max}} = 2\frac{E_0}{E_c}$$

Examples of EM showers

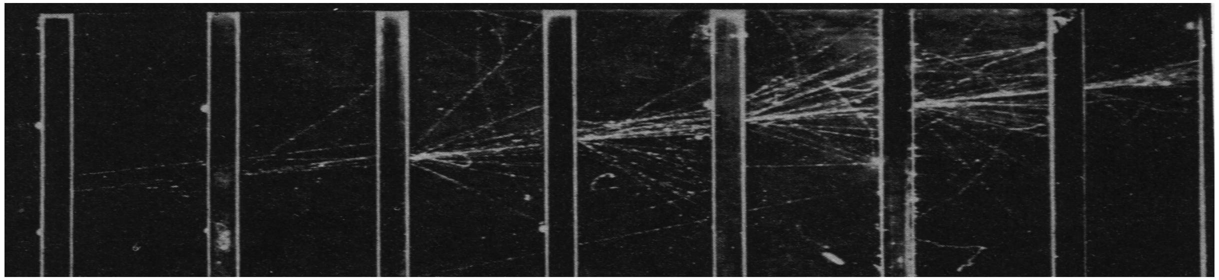

Electron shower in a cloud chamber with lead absorbers

Massive shower in a tungsten cylinder (outlined in green) produced by a single 10 GeV incident electron.

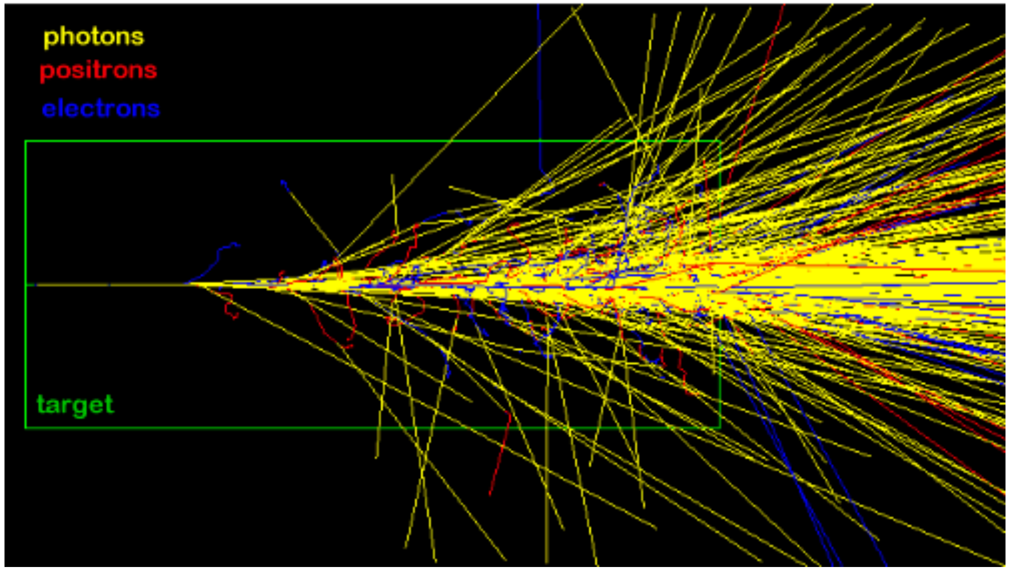

Longitudinal shower profiles

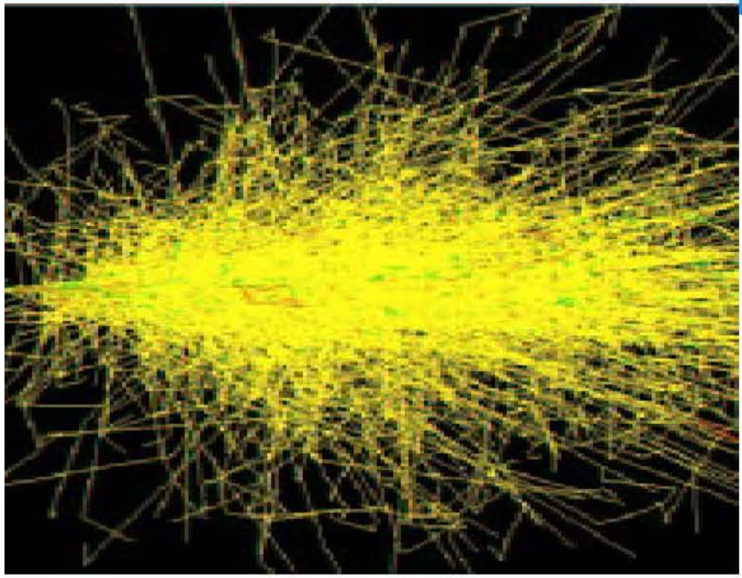

Simulation of 1 GeV electron in copper

- Multiplication of e/γ up to max shower depth where most particles reach E_c
- Exponential fall off of the shower afterwards
- Maximum shower development ~6 X_0
- Quasi universal behavior wrt X_0 but :

- Shower maximum deeper at high Z

- Slower decay at high Z

→Critical energy ∝ 1/Z

The depth of a calorimeter goes as ln(E)

Longitudinal Development EM Shower

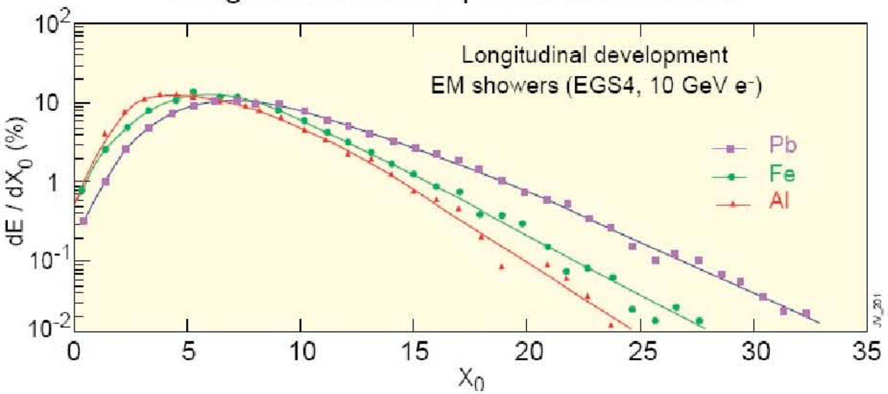

After 25 X_0 only 1% leakage for E up to 300 GeV → compact detectors!

Lateral shower profiles

- Momentum transfer → change in direction (Rutherford scattering formula)
- If the material is thick enough → multiple scattering, effect on average null for many particles but seen as a fluctuation (important for position resolution)

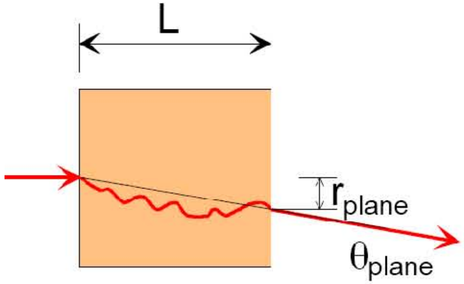

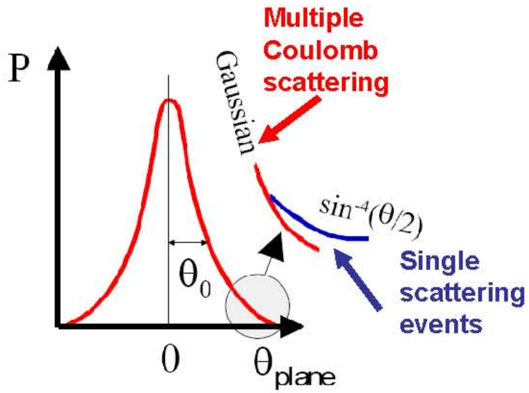

rms is given by:

$$\theta_0 = \frac{13.6\,MeV}{E} z \sqrt{\frac{L}{X_0}} \left\{ 1 + 0.038 \ln\left(\frac{L}{X_0} \right) \right\}$$

→ **Smaller for high E, small material thickness and large X_0.**

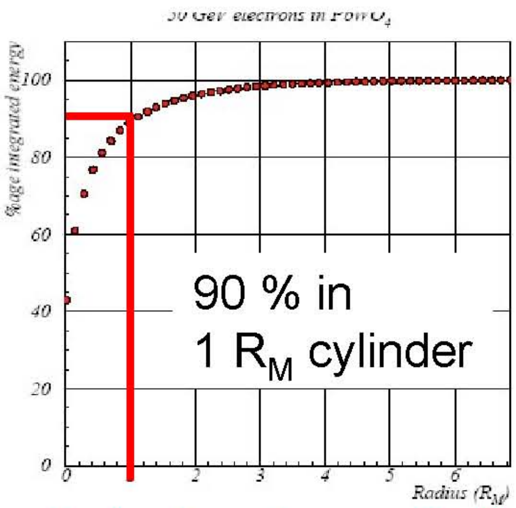

Moliere Radius (R_M): average lateral deflection of electron with E_c after 1 X_0

$R_M = 0.0265\, X_0 (Z+1.2)$

Important parameter for shower separation!

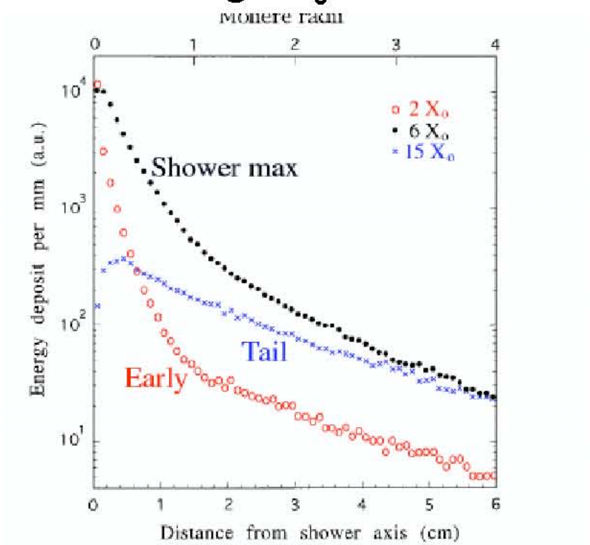

Calorimeter cell sizes should be <R_M for position measurements!

Energy resolution

Usually parameterized by :

$$\frac{\sigma}{E} = \frac{a}{\sqrt{E}} \oplus \frac{b}{E} \oplus c$$

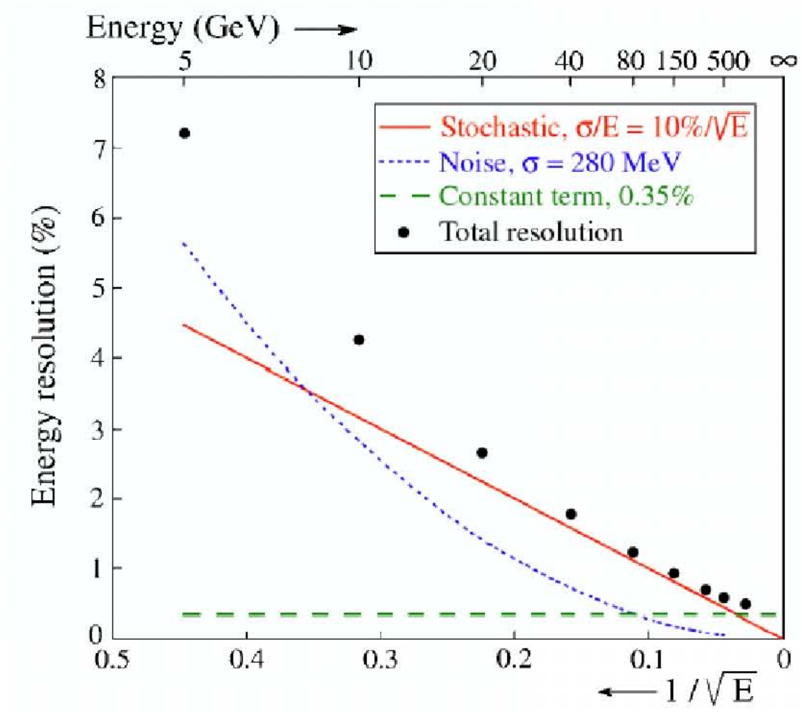

a : intrinsic resolution or stochastic term
→ given by technology choice
b : contribution of noise:
material, electronics, pile up, radioactivity
→ give by the electronics design
c : constant term: contains all the imperfection
response variation versus position (uniformity), time (stability), temperature….
→ Constraints on all aspects : mechanics, electronics….

Homogenous calorimeters: noise and constant term dominate
Sampling calorimeters: stochastic term dominates

➔ Energy resolution improves with energy compared to tracking detectors, where the momentum measurement degrades at high momentum ($dp/p \propto p$)

Homogenous crystals

In crystals the light emission is related to the crystal structure of the material. Incident charged particles create electron-hole pairs and photons are emitted when electrons return to the valence band.

The incident electron or photon is completely absorbed and the produced amount of light, which is reflected through the transparent crystal, is measured by photomultipliers or solid state photon detectors.

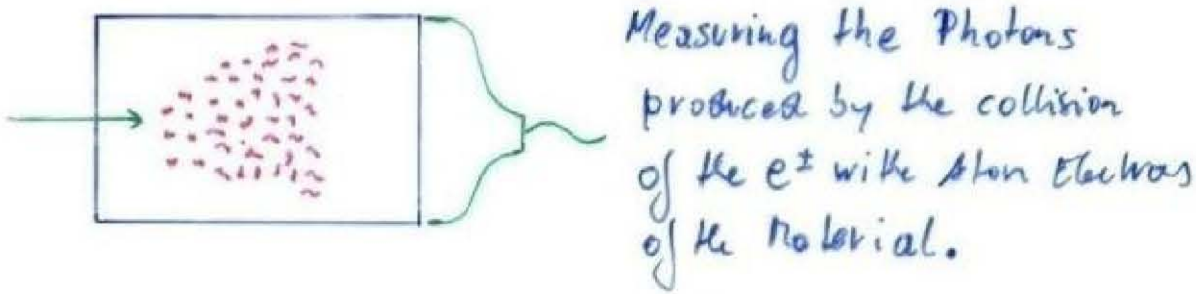

+ very compact calorimeter
+ good energy resolution
+ can be rad hard

- Crystals are not uniform by construction
- Stability: transparency, temperature sensitivity
- No longitudinal segmentation, and limited laterally
- “expensive”

Crystals used for em calorimeters

Crystal	NaI(Tl)	CsI(Tl)	CsI	BaF_2	BGO	CeF_3	$PbWO_4$
Density $g.cm^{-2}$	3.67	4.51	4.51	4.89	7.13	6.16	8.28
Rad. length cm	2.59	1.85	1.85	2.06	1.12	1.68	0.89
Moliére radius cm	4.5	3.8	3.8	3.4	2.4	2.6	2.2
Int. length cm	41.4	36.5	36.5	29.9	22.0	25.9	22.4
Decay Time ns	250	1000	35 6	630 0.9	300	10-30	<20>
Peak emission nm	410	565	420 310	300 220	480	310- 340	425
Rel. Light Yield %	100	45	5.6 2.3	21 2.7	9	10	0.7
d(LY)/dT $\%/^0C$	≈ 0	0.3	- 0.6	- 2 ≈ 0	- 1.6	0.15	-1.9
Refractive Index	1.85	1.80	1.80	1.56	2.20	1.62	2.16

Belle/ Babar: 10ms interaction rate, good light yield, good S/N

L3: 25µs bunch crossing, low radiation dose

CMS/ Alice: 25ns bunch crossing, high radiation dose

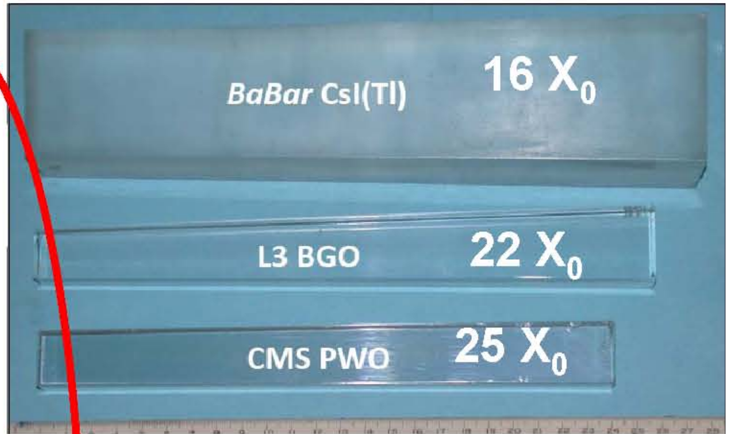

Need to match crystal with photo-detector

Shower profiles in $PbWO_4$

Simulation of longitudinal shower profile **Simulation of transverse shower profile**

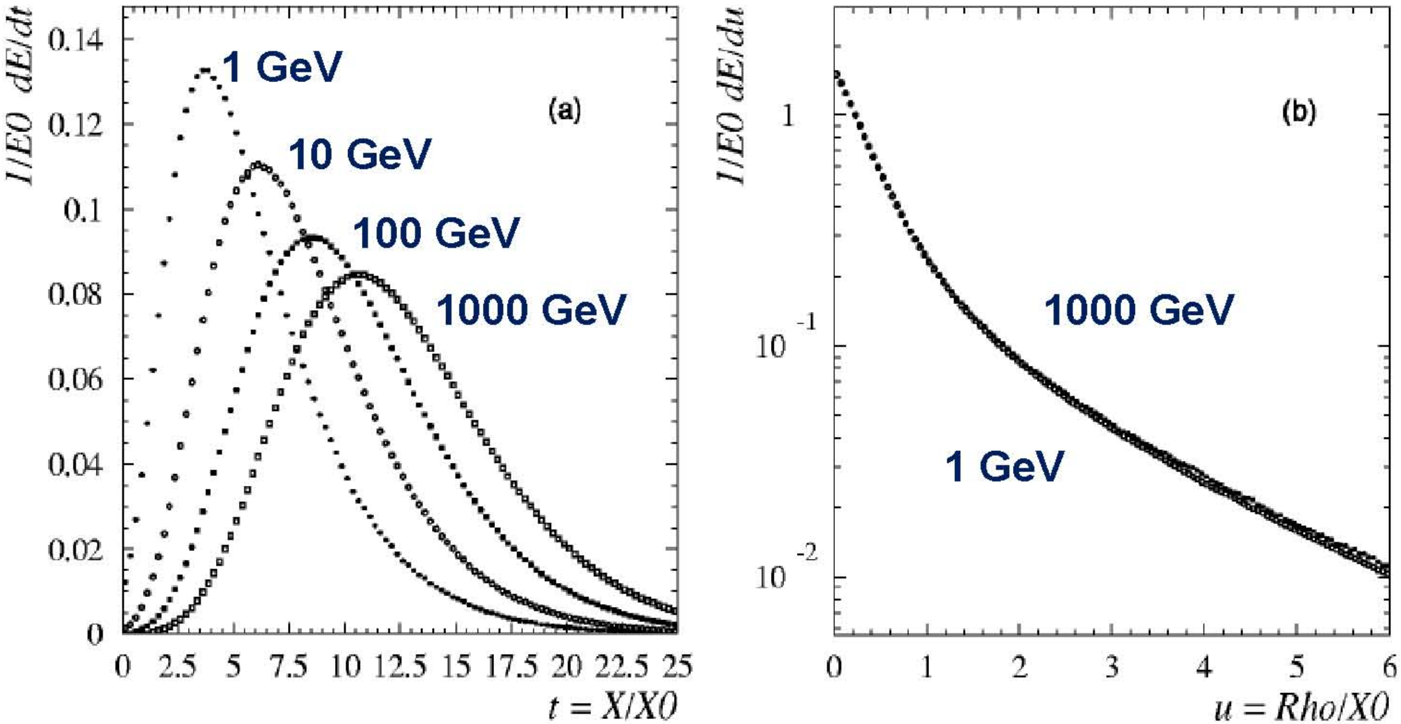

FIG. 2. (a) Simulated shower longitudinal profiles in $PbWO_4$, as a function of the material thickness (expressed in radiation lengths), for incident electrons of energy (from left to right) 1 GeV, 10 GeV, 100 GeV, 1 TeV. (b) Simulated radial shower profiles in $PbWO_4$, as a function of the radial distance from the shower axis (expressed in radiation lengths), for 1 GeV (closed circles) and 1 TeV (open circles) incident electrons. From Maire (2001).

CMS crystal em calorimeter

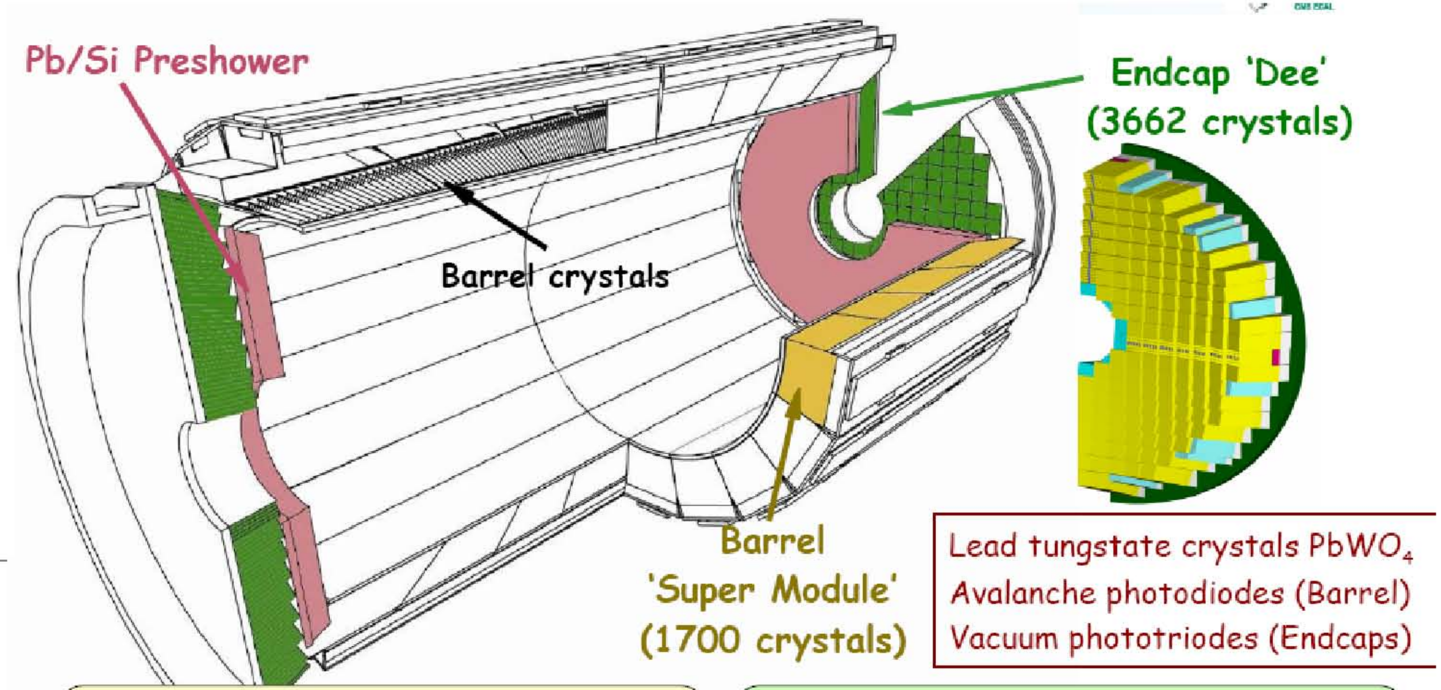

Excellent stochastic term
Challenge: uniformity/stability
→constant term

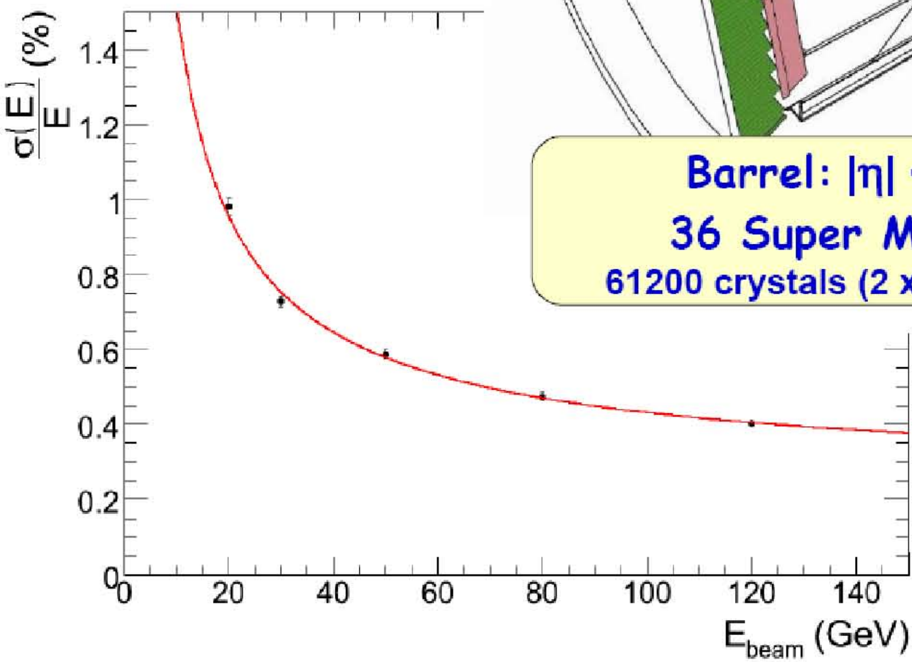

Barrel: |η| < 1.48
36 Super Modules
61200 crystals (2 x 2 x 23 cm^3)

Endcaps: 1.48 < |η| < 3.0
4 Dees
14648 crystals (3 x 3 x 22 cm^3)

$$\left(\frac{\sigma}{E}\right)^2 = \left(\frac{3.37\%}{\sqrt{E}}\right)^2 + \left(\frac{0.107}{E}\right)^2 + (0.25\%)^2$$

Stochastic Noise Constant

inside a crystal

Sampling calorimeters

Use a different medium to generate the shower and to detect signal

Sampling Fraction =
Energy deposited in Active/
Energy deposited in passive material.

$$f_{samp} = \frac{E_{mip}(actif)}{E_{mip}(actif) + E_{mip}(absorbeur)}$$

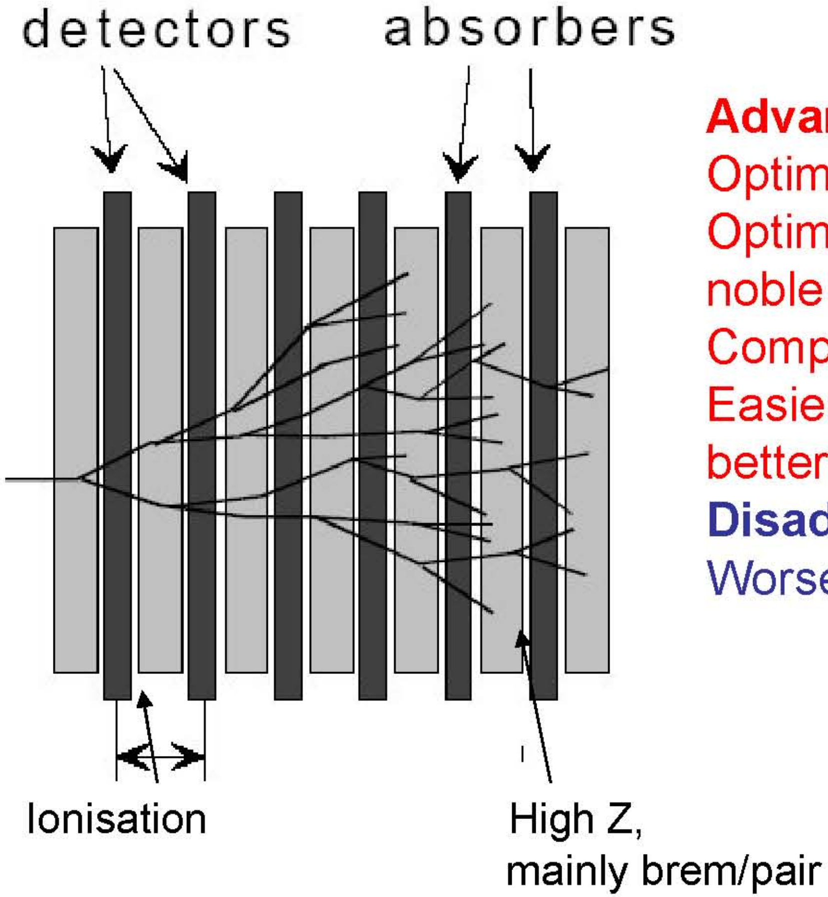

Advantage:
Optimum choice of absorber materiel (Pb, Ur, W, Fe)
Optimum choice of detector material (scintillator, noble liquid, gas or solid state detectors)
Compact and cheap construction
Easier segmentation➔ better space resolution, better particle identification

Disadvantage:
Worse resolution → larger stochastic term

$$\frac{\sigma(E_M)}{E_M} = a\sqrt{\frac{d}{f_{samp}}}\frac{1}{\sqrt{E}} \approx \frac{5-20\%}{\sqrt{E}}$$

Liquid sampling calorimeter

The active material is generally a noble liquid

➔ need for cryogenic temperatures

Warm liquids work at room temperature exists, have poor radiation resistance and suffer from purity problems

➔ operation in 'ion chamber mode', i.e. deposited charge is large and doesn't need multiplication:

better uniformity compared to gas calorimeters that need amplification.

➔ relatively uniform and easy to calibrate because the active medium is homogeneously distributed inside the volume.

➔ good energy resolution and stable operation with time.

➔they are radiation hard.

➔ rather slow…

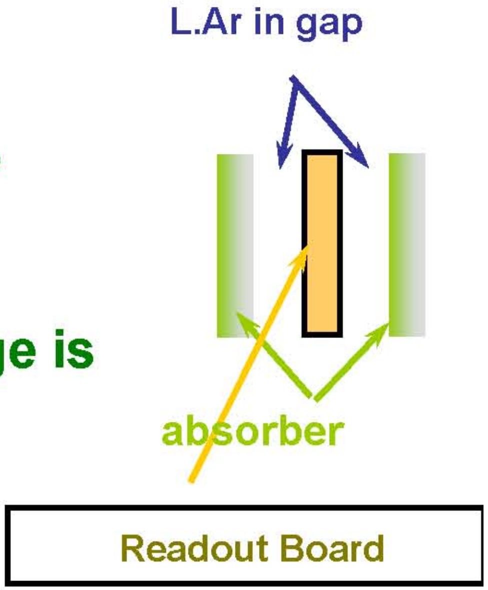

Noble liquids for em calorimeters

	Ar	Kr	Xe
Z	18	36	58
A	40	84	131
X_0 (cm)	14	4.7	2.8
R_M (cm)	7.2	4.7	4.2
Density (g/cm^3)	1.4	2.5	3.0
Ionization energy (eV/pair)	23.3	20.5	15.6
Critical energy ϵ (MeV)	41.7	21.5	14.5
Drift velocity at saturation (mm/μs)	10	5	3

- charge particle convert about half of their lost energy into ionization and half into scintillation.
-best energy resolution if collecting both the charge and light signal!
- but rather difficult to extract light and charge in the same instrument…

Liquid Argon, 5mm/ µs at 1kV/cm, 5mm gap:
➔ 1 µs for all electrons to reach the electrode
➔ 0.1ms for ions ! → don't contribute to the signal for electronics of µs integration time.

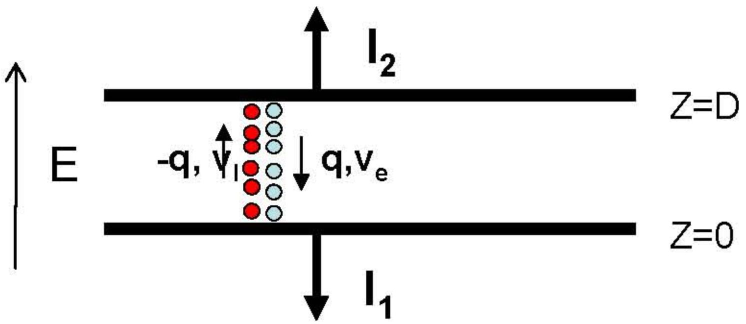

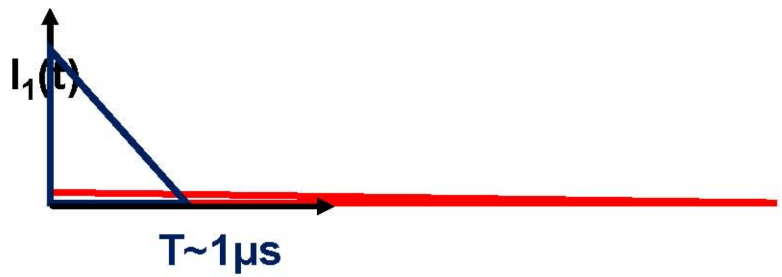

Atlas liq Argon em calorimter

Standard liquid argon calorimeters: absorber and active layers are perpendicular to the direction of the incident particle.
→Long cables needed to gang together the readout electrodes
→ signal degradation, dead spaces between the calorimeter towers
➔ reduced hermeticity.

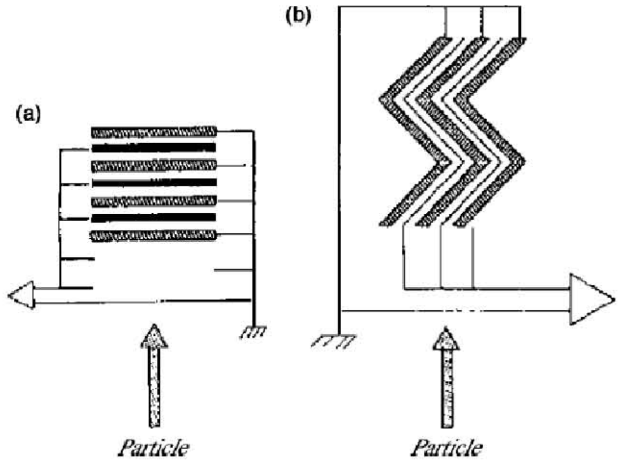

FIG. 15. Schematic view of a traditional sampling calorimeter geometry (a) and of the accordion calorimeter geometry (b).

ATLAS LAr Calorimeter: absorbers in an accordeon geometry parallel to the particle direction ➔ electrodes can easily be read out from the 'back side'.

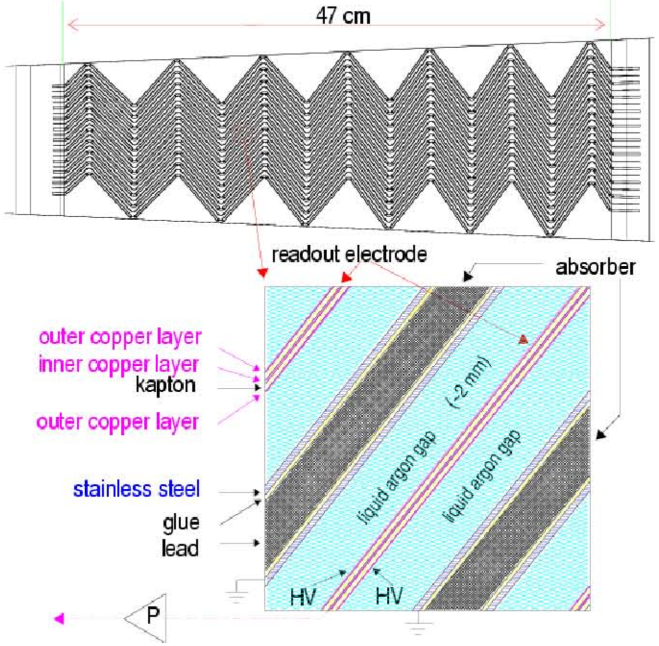

Summary so far:

Electrons, positrons and photons give rise to electromagnetic cascades in a calorimeter

- The shower depth increases only like ln$E$.
- Laterally contained to 90% in 1R_M

The shower is measured in homogeneous or sampling calorimeters.

(Pros and cons for both.

Take 5 mins to discuss in groups of 4).

This section:

- Hadronic cascades
- Hadronic compensation
- Signal treatment and calibration
- Resolution
- Examples of (expected) performances

Towards the end we will discuss
- Clustering, jets
- Jet substructure
- Particle flow

EM and Hadronic showers

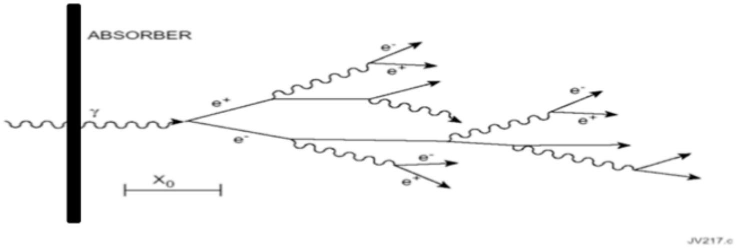

EM

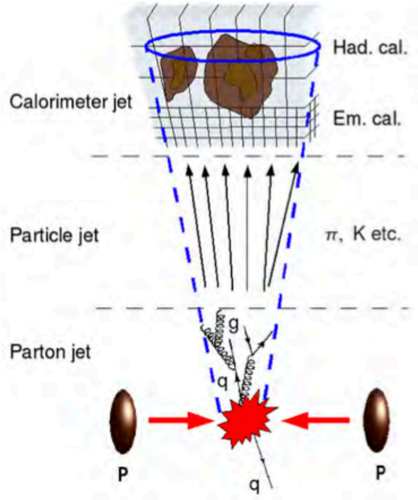

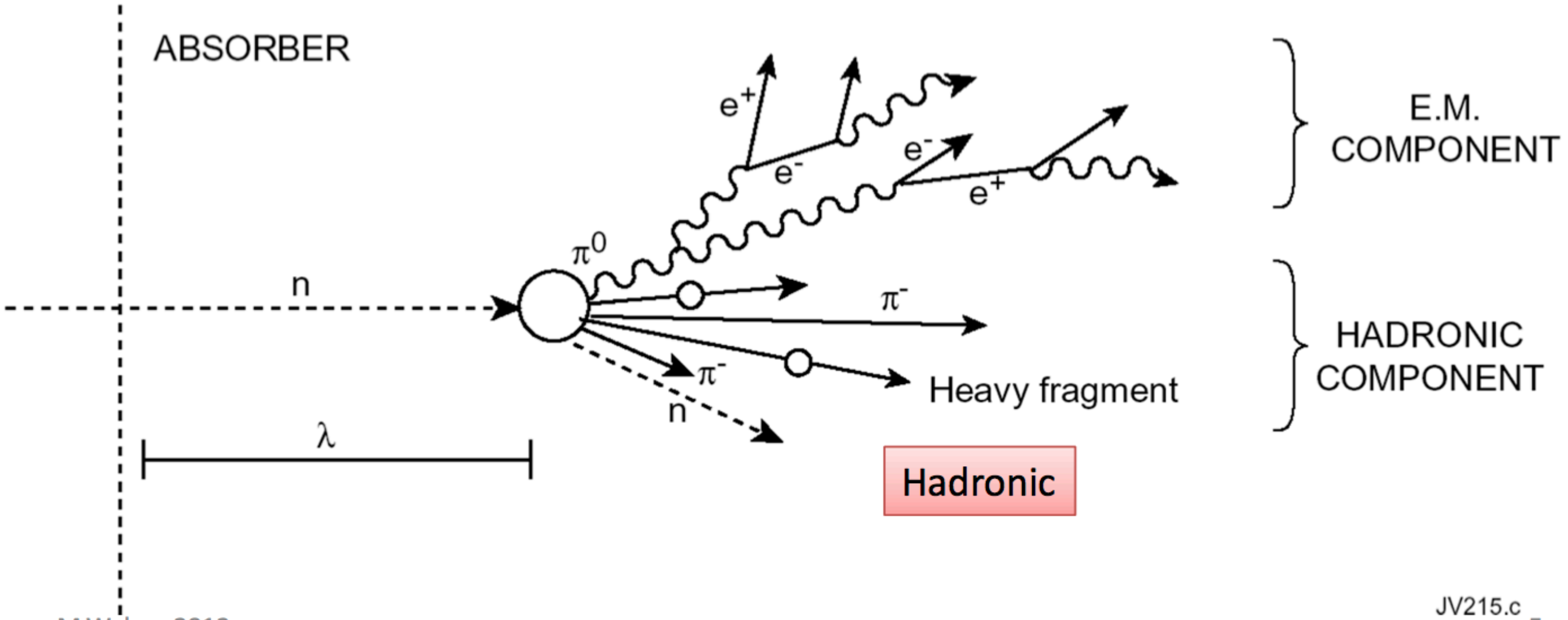

Hadronic

Hadron showers

1. **Production of energetic secondary hadrons**
   - Number of particles produced ~ ln (E) with an "interaction length" $\lambda \approx 35\, A^{1/3}$
   - secondary particles produced: p, n, $\pi^{+/-}$,and
     $\pi^0 \rightarrow 2\gamma \rightarrow$ electromagnetic component of the hadron shower
   - Hadrons thermalize but only <10% energy loss through ionization
2. **Nuclear interactions ➔ resulting in a few MeV photons**
   - Produced slowly ~μs ➔ mostly invisible energy

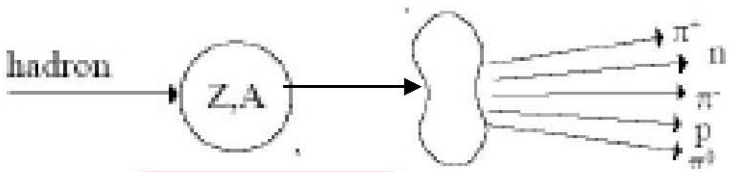

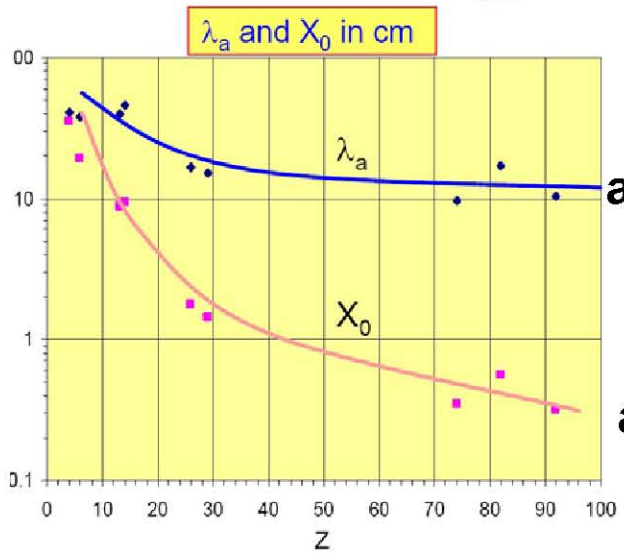

as $A^{1/3}$

as A/Z^2

Proton on lead

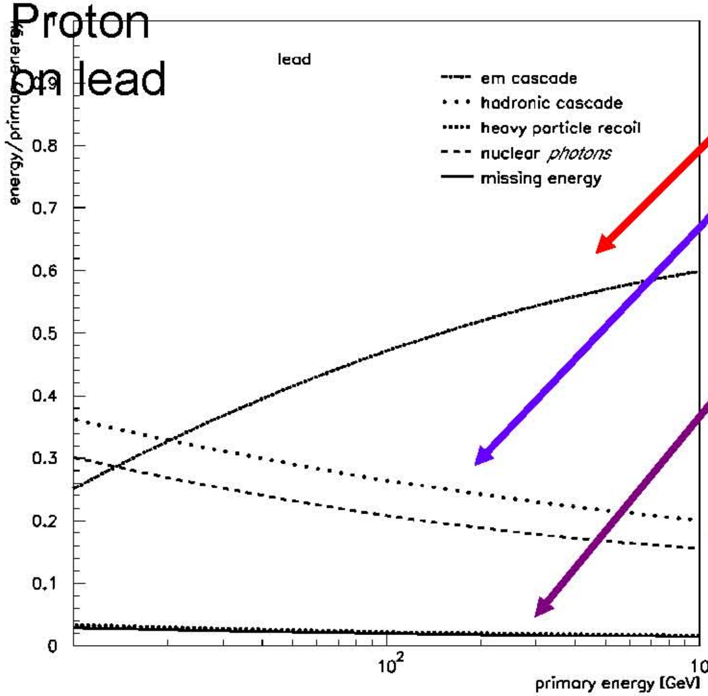

em component

hadronic cascade

ν from heavy quark and μ decays

invisible energy

Resolution for hadron calorimeters

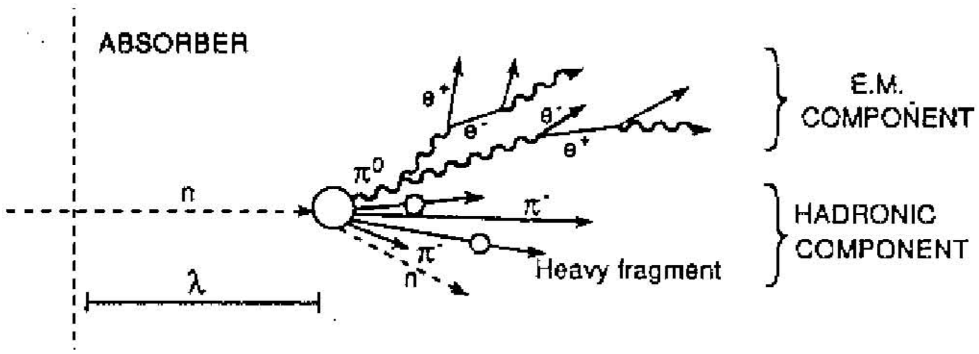

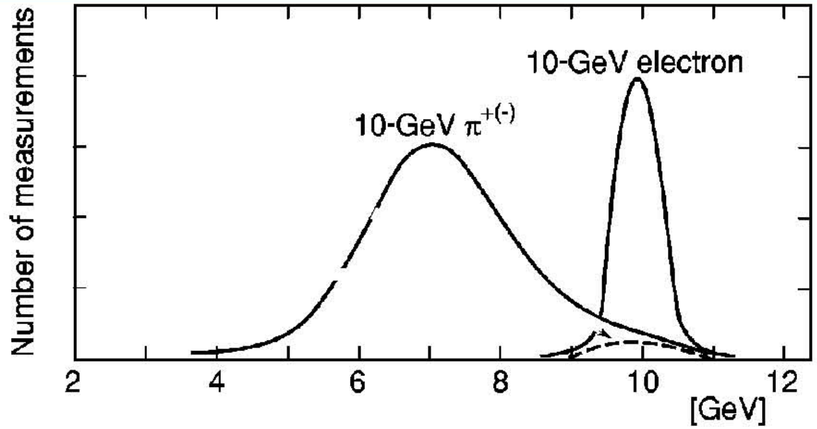

Signal (in energy units) obtained for a 10 GeV energy deposit

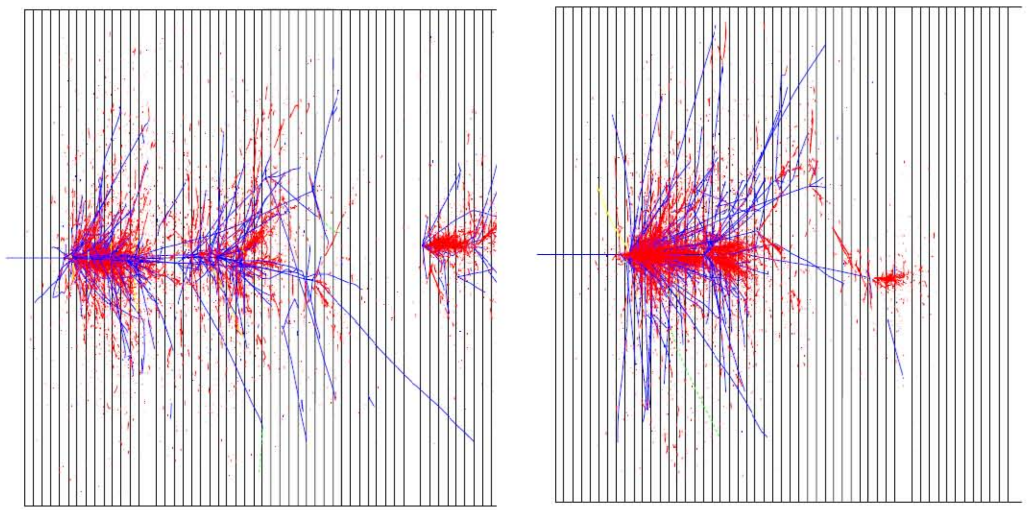

red: em component   blue: hadronic component

- **not all the incident energy is measured : e/π > 1**
- very large event to event fluctuations between hadron and em component
- em component energy dependent→ non linear →resolution worse than for em showers!

Typical resolutions: $$\frac{\sigma(E)}{E} \approx \frac{50-100\ \%}{\sqrt{E}} \oplus 3-5\% \text{ (E en GeV)}$$

Recombination and quenching effects may reduce signals in calorimeters

- Depends on dE/dx

$$\mathit{Birk's\ law:}\quad \frac{dL}{dx} = L_0 \frac{\frac{dE}{dx}}{1 + kB\frac{dE}{dx}}$$

Compensation for hadron calorimeters

e/π ratio is a major component to the resolution !
- if e/π ≈ 1 the calorimeter is « compensated »

How to achieve compensation?
- impossible to have a similar response to e and hadrons in a homogenous calorimeter
- sampling calorimeters allow to optimize absorber and active materialfor the hadron cascade,
- active material containing hydrogen (Scintillator) sensitive to neutrons!
- long integrations times…

- **High Z absorber material: U, Pb, but difficult due to mecanical constraints**

- Tuning of the thickness between absorber and active material!

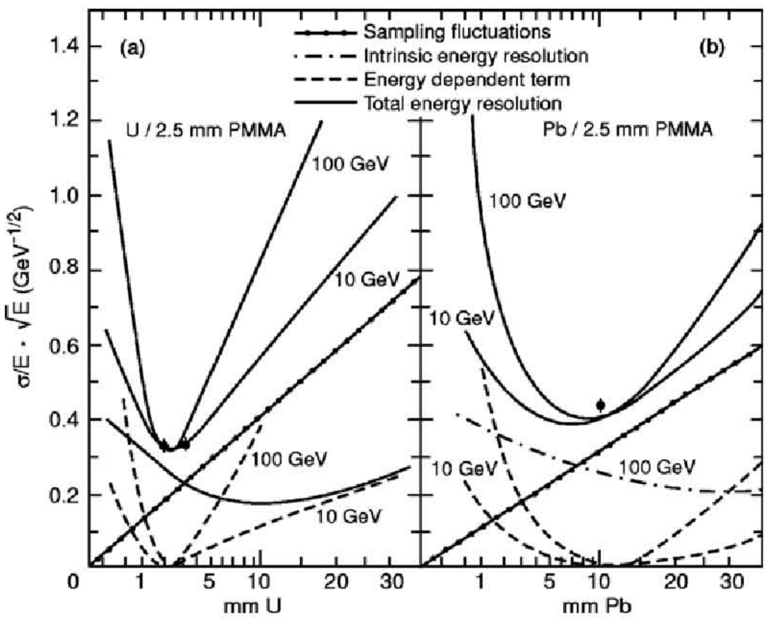

Shower profiles

300 GeV pion, 95% in 8 λ_{int} (85 cm of U)
300 GeV electron , in 30 X_0 (Pb 9cm)

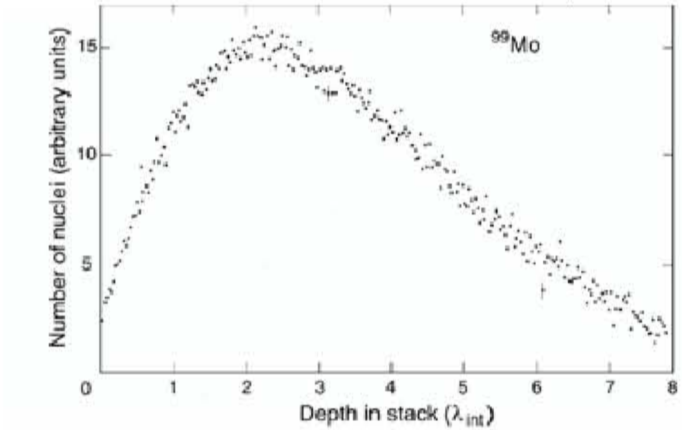

80 GeV pion, 95% in 1.5 λ_{int} (32 cm)
80 GeV electron (3.5cm)

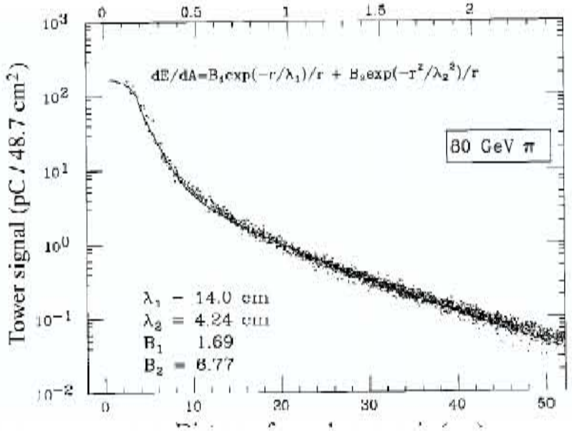

- typically factor ~10 on shower sizes, shower max at ~2λ

➔a large energy fraction of the hadron shower is in the em sections !

peak of events starting to shower in e.m. calo.

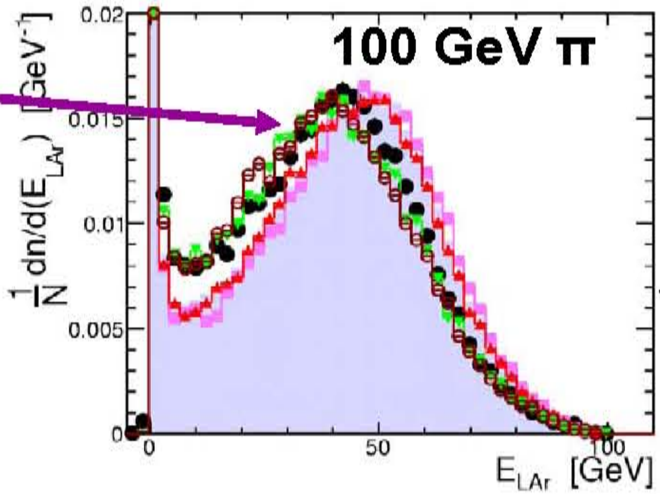

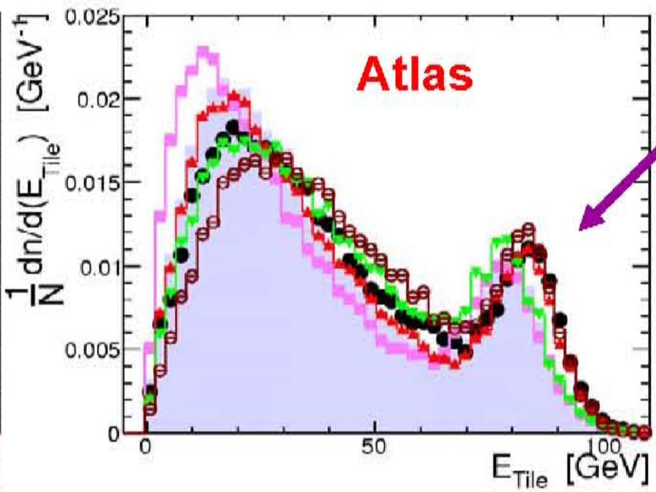

peak of events starting to shower after e.m. calo.

HCal generalities

- All the hadronic sections of the hadron collider experiments are sampling calorimeters
  - Possible optimization of e/π response, yet limited resolution of hadron showers
  - Jet radius rather large: coarser granularity, fewer longitudinal segmentation
  - big devices: mechanical considerations, cost consideration
  - Energy fraction deposited decreases with depth, radius of the device increases: less performing absorber material at the outside

  ➔ use of robust and rather cheep absorber material

  ➔ active material: either liquid Argon or scintillator

Tile calorimeters

• Atlas barrel HCAL : l=5.6m r=4.2m
• iron/scintillating tiles
• 10K readout channels in 3 layers (1.4λ, 3.9λ, 1.8λ, ~2λ from em) with a η x φ segmentation of 0.1x0.1 – except last layer 0.2x0.1 (TC)
• resolution: $\sigma/E=50\%/\sqrt{E} \oplus 3\%$

CMS: barrel HCAL: l=9m, r=6m
• brass-scintillator calorimeter
• 10k channels 5.2λ (10λ total) with a η x φ segmentation of 0.087x0.087
• HO: scintillator array in the central region outside the magnet to catch leakage energy
•resolution: $\sigma/E=100\%/\sqrt{E} \oplus 4\%$

D0 - Calorimeter

- **4-5 hadronic layers (FH + CH)**
- **Uranium absorber in EM and Uranium-Nobium in FH**
- **Cu (CC) or Steel (EC) for coarse hadronic**

From test beam measurments:

- **compensating e/π ~ 1 for Run I intergration time**

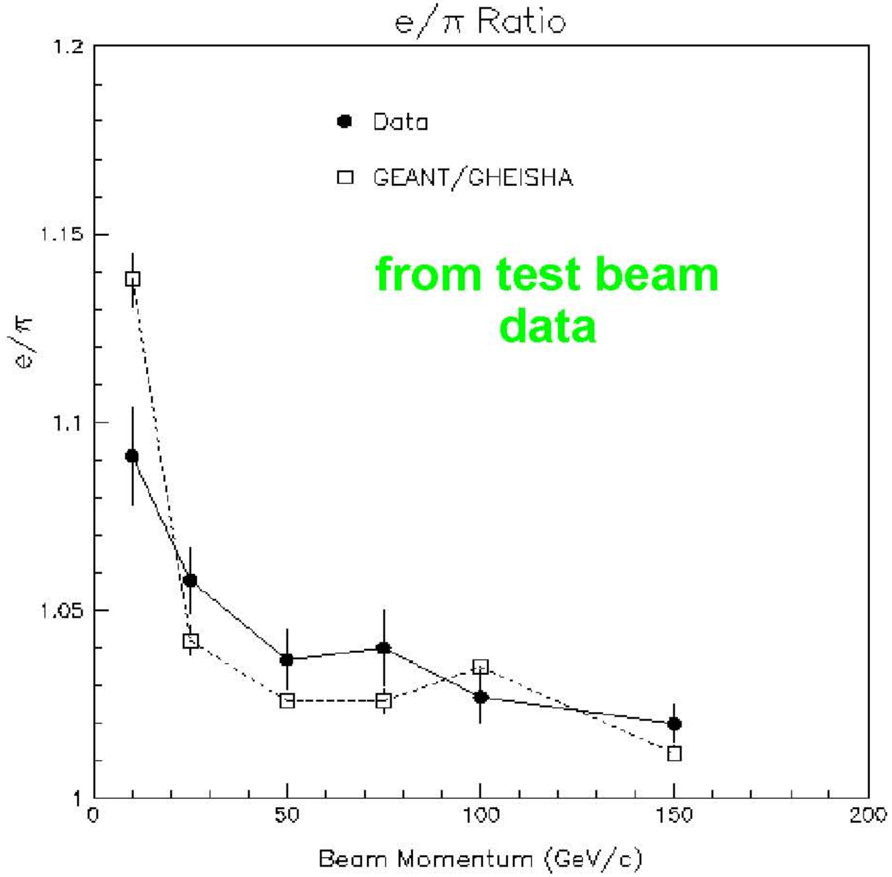

e: $\sigma_E/E = 15\% /\sqrt{E} + 0.3\%$

π: $\sigma_E/E = 45\% /\sqrt{E} + 4\%$

Signal treatment and calibration

Example: ATLAS Barrel EM calorimeter.

~2mm Lar gap ➔ e^- drift time ~400 ns
Too long compared to LHC clock (25 ns) ➔ use bipolar shaping

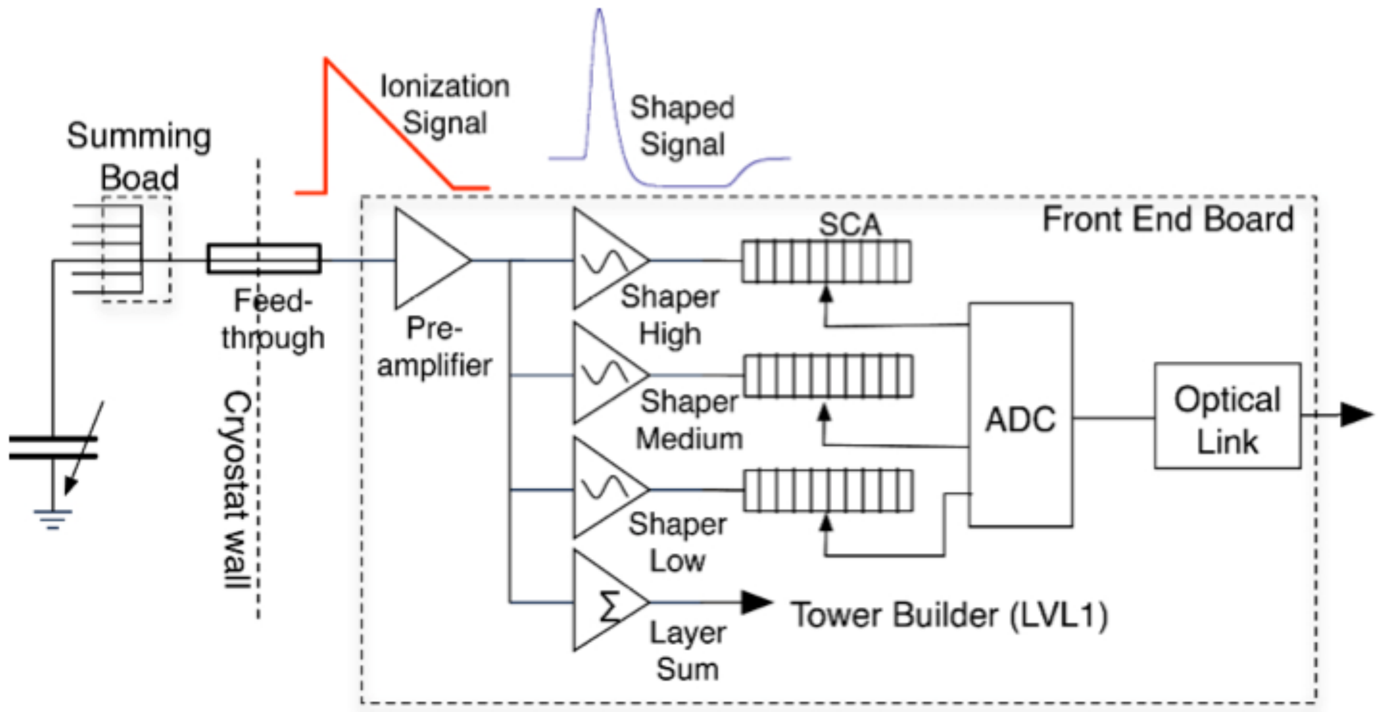

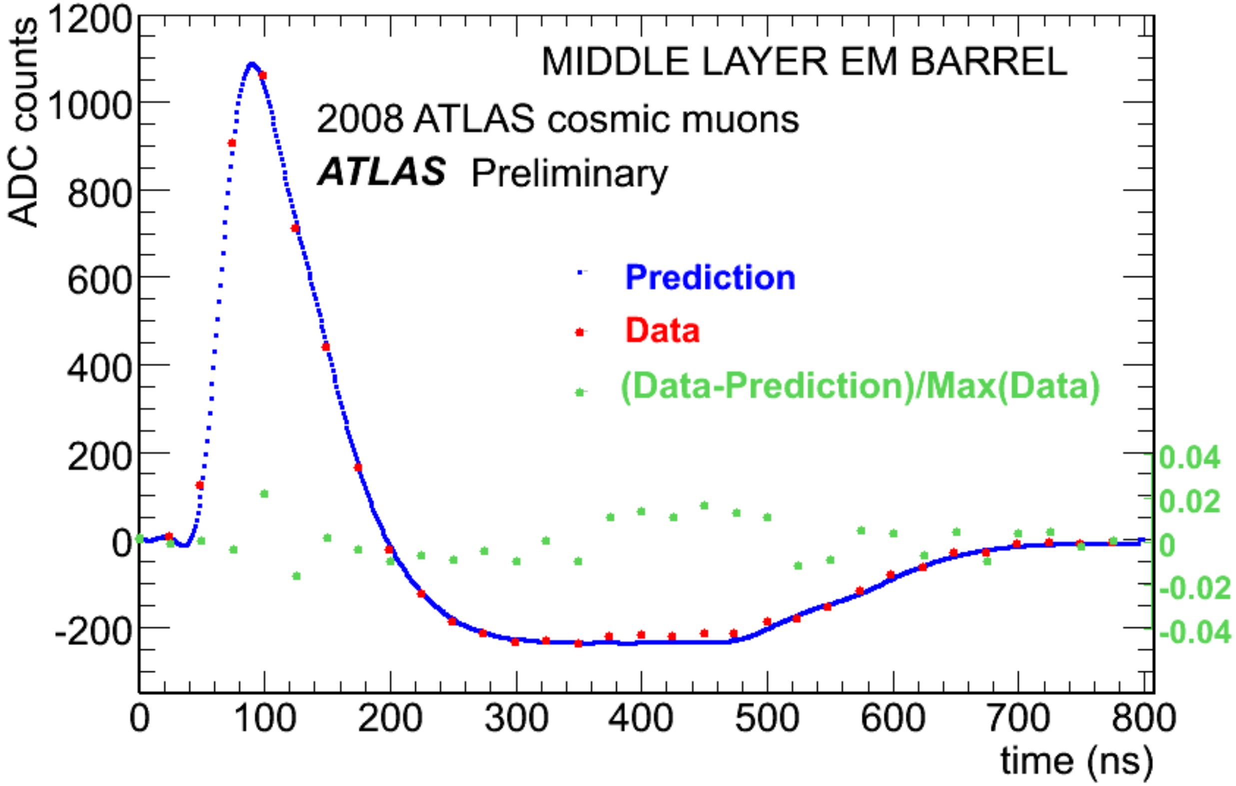

- Measure amplitude every 25 ns (LHC clock).
- Each measurement contains information about the pulse height provided the pulse shape and phase of the measurement is known.

Optimal filtering: amplitude A and time τ are obtained from

$$A = \sum_{i=1}^{5} a_i (s_i - p) \qquad A\tau = \sum_{i=1}^{5} b_i (s_i - p)$$

Where the optimal filtering coefficients a_i and b_i are computed from the pulse shape and the noise autocorrelation function. p is the pedestal and s_i the sampled signa.l

KTH Engineering Sciences

Calibration

With electronic pulses:

- The pedestal is measured in “empty” pulse triggers
- Pulses of different amplitudes are injected before preamplifiers (e.g on summing boards)
- Shape of the pulse from the electronics chain can be obtained by delaying the pulse compared to the ADC clock.

A conversion factor to energy is obtained from test beam measurements with electrons (starting from a calculated factor from charge to current conversion and relation to test pulse).
The conversion factor can be improved from e.g. Z ➔ ee

This defines the electromagnetic (EM) scale

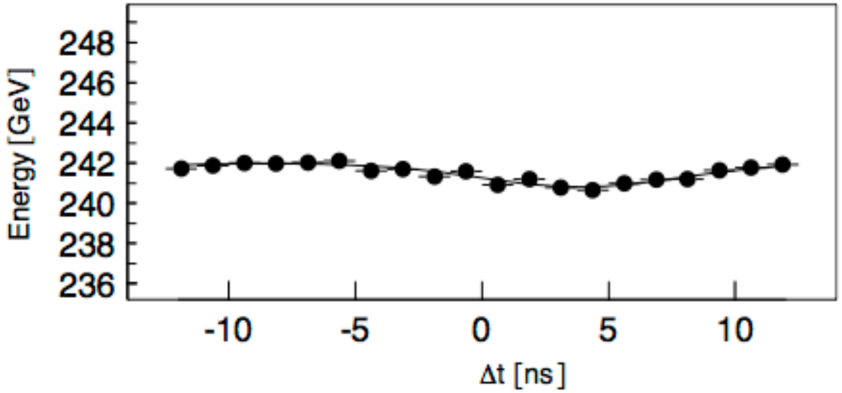

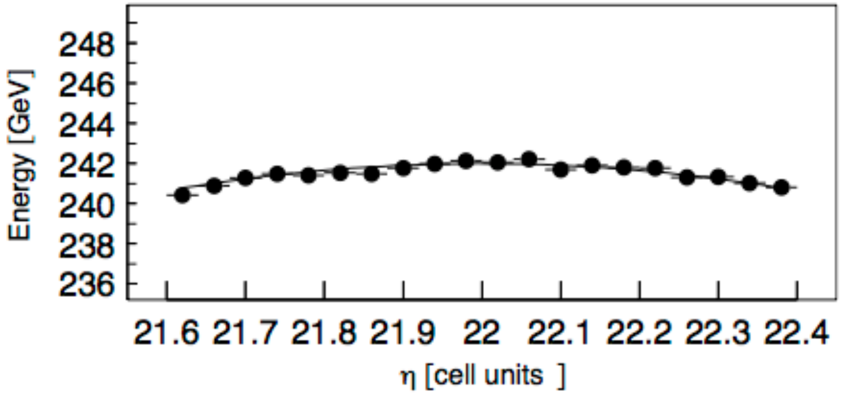

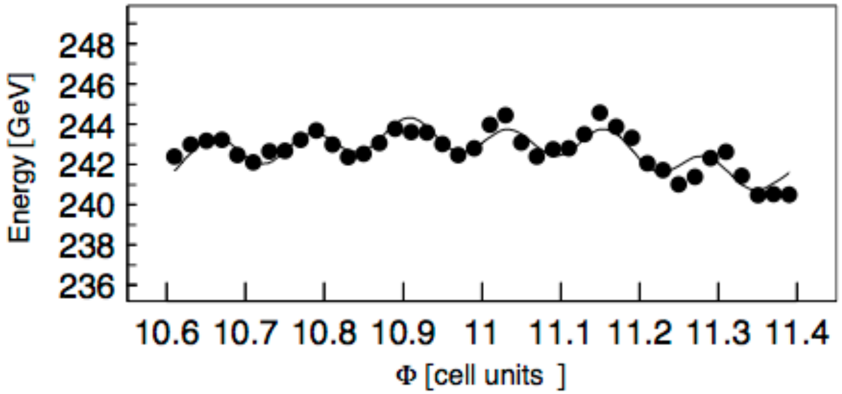

ATLAS EM barrel (Module 0)

Corrections can be applied for

- Phase of pulse compared to readout clock

- Finite cluster size (3 x 3 EM cells)

- φ modulation due to accordion shape. 4 accordion shaped electrodes per φ cell

KTH Engineering Science

ATLAS EM barrel (Module 0)

Energy resolution at different η

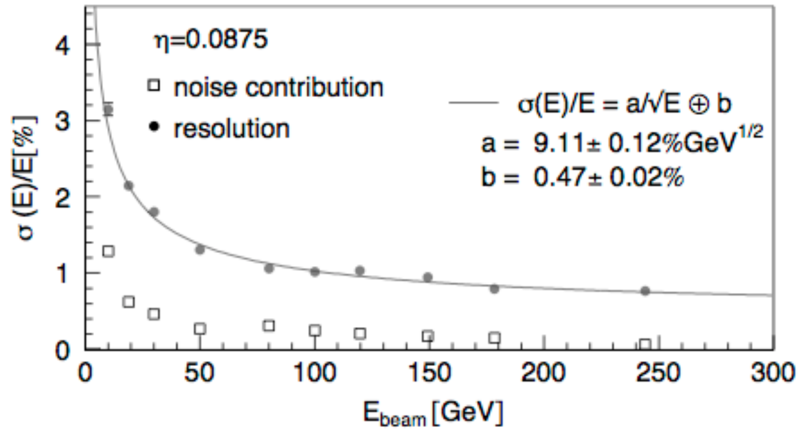

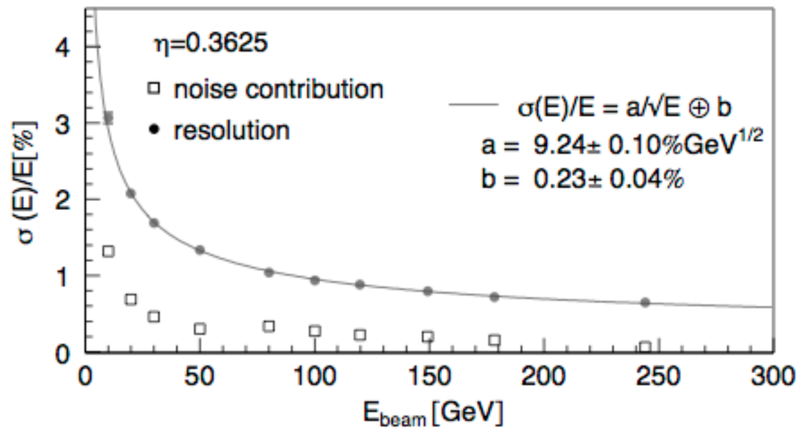

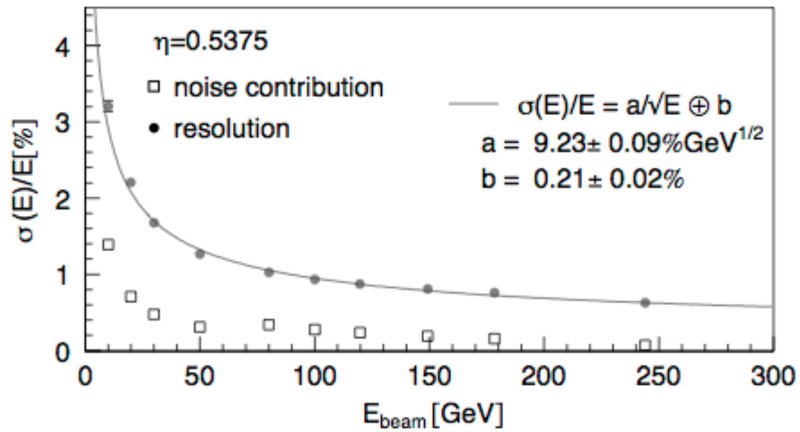

KTH Engineering Sciences

ATLAS EM barrel (Module 0)

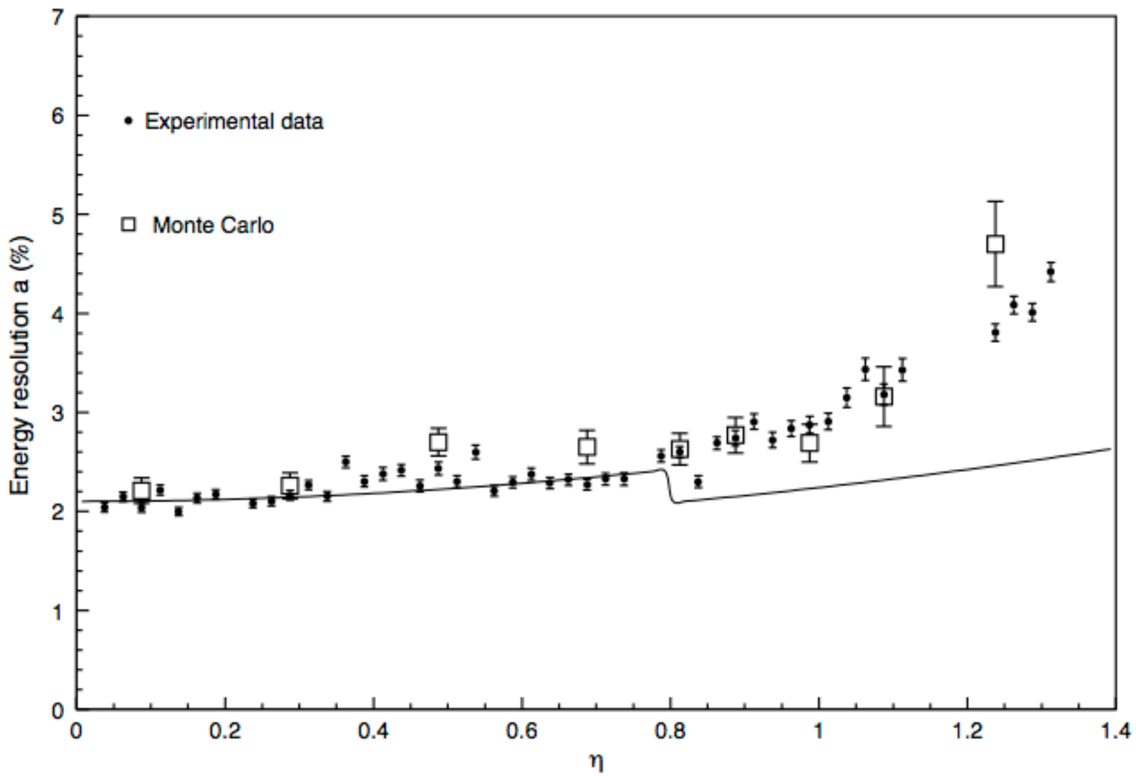

Fig. 25. Energy resolution as a function of rapidity, as obtained with an electron beam of 20 GeV. The curve shows the geometrical expectation, normalized at $\eta = 0$ and rescaled at $\eta = 0.8$ with the square root of the ratio of the two lead thicknesses.

Sampling frequency changes with the angle.

Position measurements

- finite size clusters are used ➔ S-shape corrections

nominal

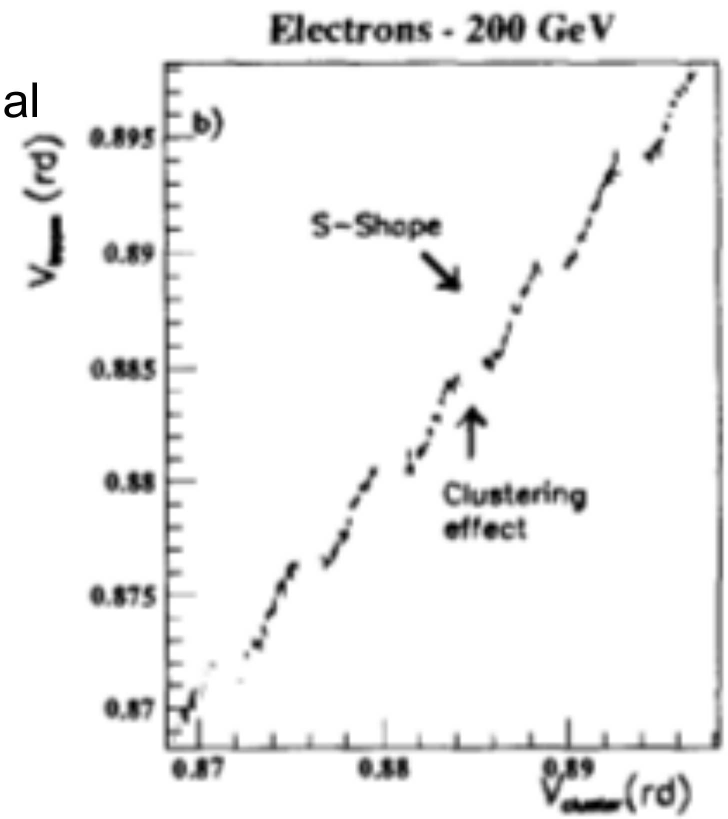

cluster

This section:

- Clustering, jets
- Jet energy scale
- Jet substructure
- Particle flow

Clustering can be based on

KTH Engineering Sciences

Towers

Sum calorimeter cells in a pointing grid in Δη x Δφ
Used for EM clusters.
Tower size depends on object and calo region

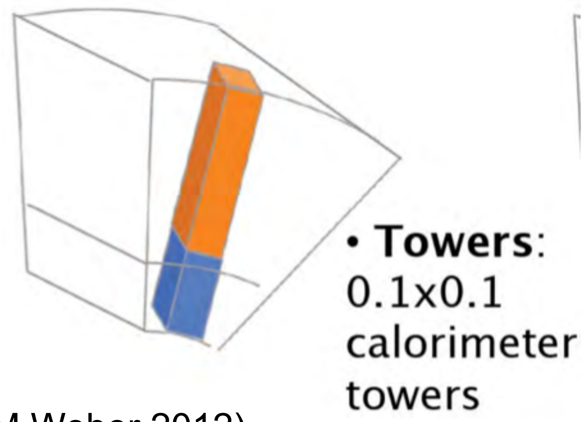

(M Weber 2012)

Topological clusters

- Use fine cell granularity
- Only add cell energies that are significant compared to expected noise. E.g.:
  - Start from seed cell with S/N > 4
  - Add all neighbouring cells with S/N > 2
  - Add direct neighbour cells with S/N > 0

  (420 topo clusters)
- There are procedures to split cell energies between overlapping clusters

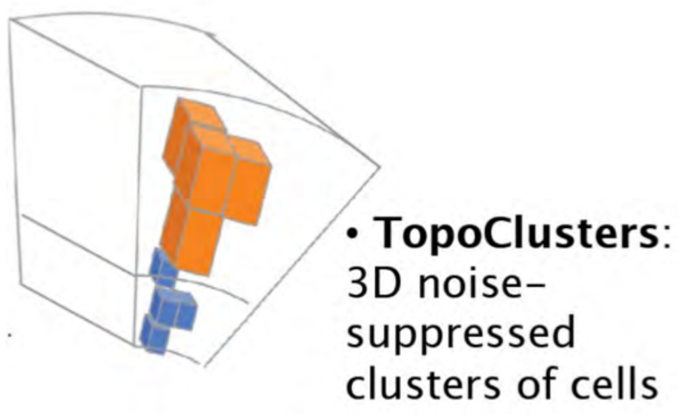

(M Weber 2012)

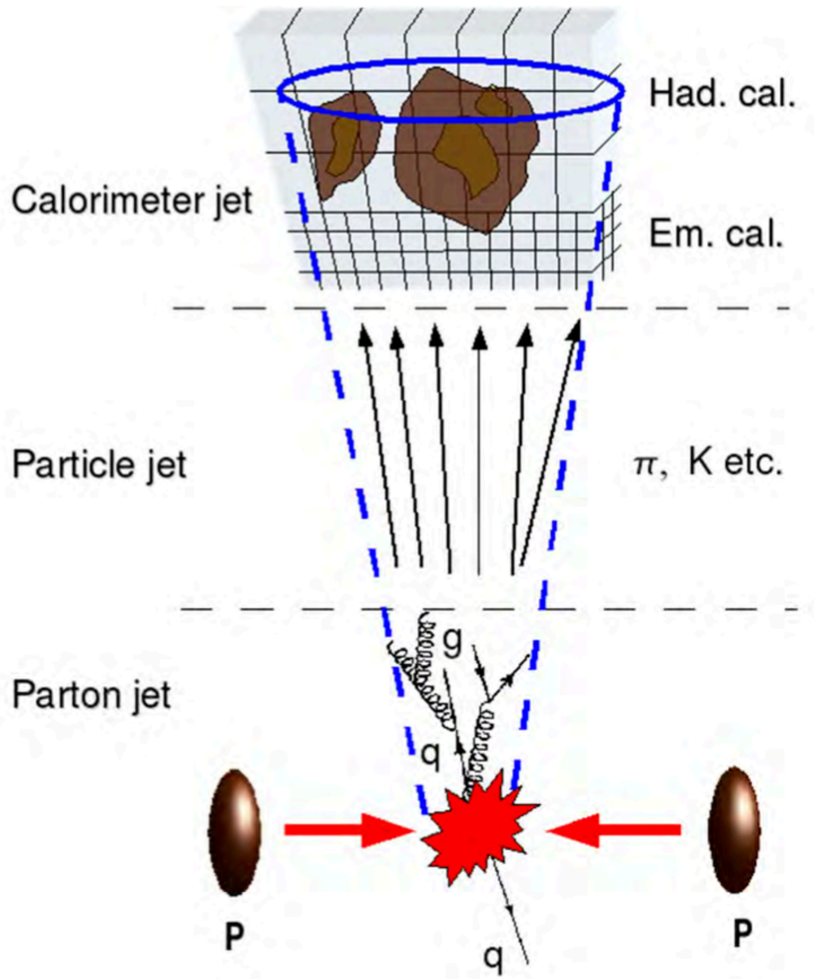
Had. cal.
Calorimeter jet
Em. cal.
Particle jet
π, K etc.
g
Parton jet
q
P
P
q

KTI

Detector Effects On Jets

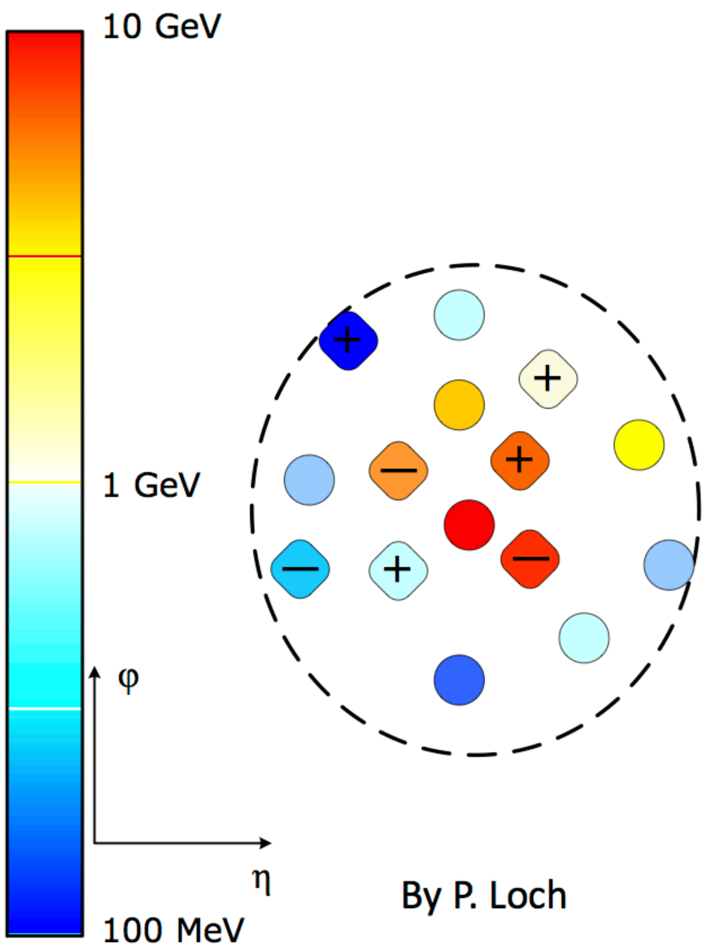

By P. Loch

Change of composition

- Radiation and decay inside detector volume
- "Randomization" of original particle content

Defocusing changes shape in lab frame

- Charged particles bend in solenoid field

Attenuation changes energy

- Total loss of soft charged particles in magnetic field
- Partial and total energy loss of charged and neutral particles in inactive upstream material

Hadronic and electromagnetic cacades in calorimeters

- Distribute energy spatially
- Lateral particle shower overlap

Detector Effects On Jets

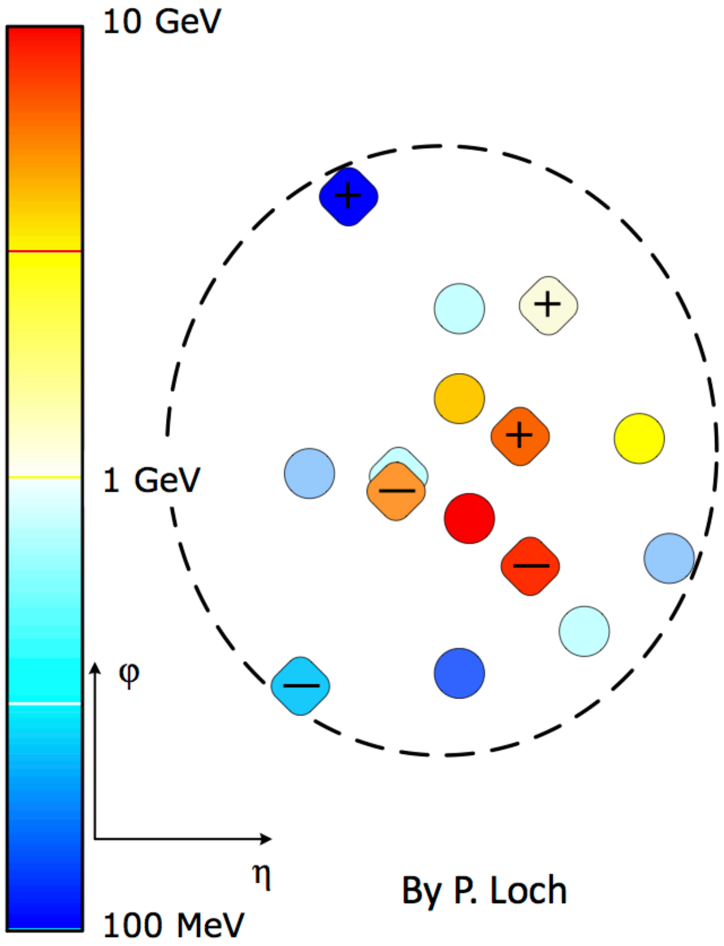

By P. Loch

Change of composition

- Radiation and decay inside detector volume
- "Randomization" of original particle content

Defocusing changes shape in lab frame

- Charged particles bend in solenoid field

Attenuation changes energy

- Total loss of soft charged particles in magnetic field
- Partial and total energy loss of charged and neutral particles in inactive upstream material

Hadronic and electromagnetic cacades in calorimeters

- Distribute energy spatially
- Lateral particle shower overlap

KTI

Detector Effects On Jets

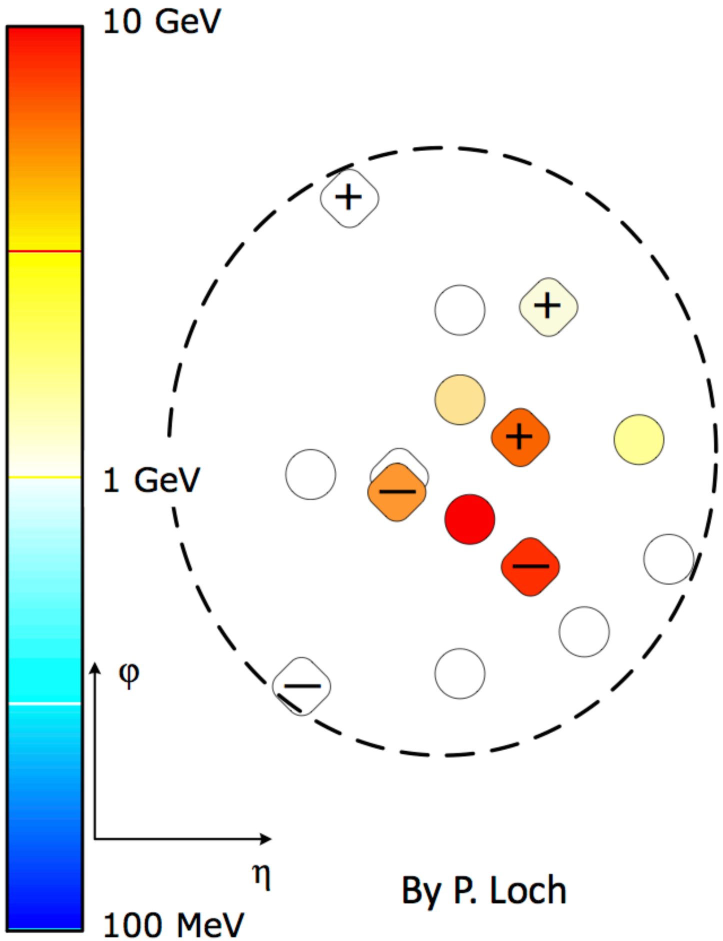

By P. Loch

Change of composition

- Radiation and decay inside detector volume
- "Randomization" of original particle content

Defocusing changes shape in lab frame

- Charged particles bend in solenoid field

Attenuation changes energy

- Total loss of soft charged particles in magnetic field
- Partial and total energy loss of charged and neutral particles in inactive upstream material

Hadronic and electromagnetic cacades in calorimeters

- Distribute energy spatially
- Lateral particle shower overlap

KTI

Detector Effects On Jets

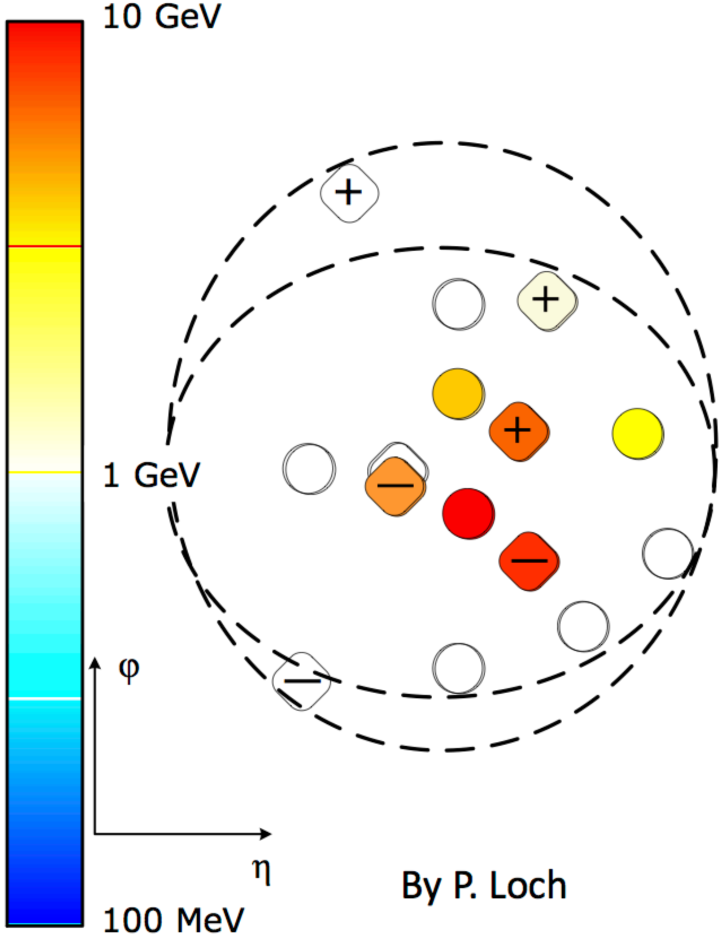

Change of composition

- Radiation and decay inside detector volume
- "Randomization" of original particle content

Defocusing changes shape in lab frame

- Charged particles bend in solenoid field

Attenuation changes energy

- Total loss of soft charged particles in magnetic field
- Partial and total energy loss of charged and neutral particles in inactive upstream material

Hadronic and electromagnetic cacades in calorimeters

- Distribute energy spatially
- Lateral particle shower overlap

Detector Effects On Jets

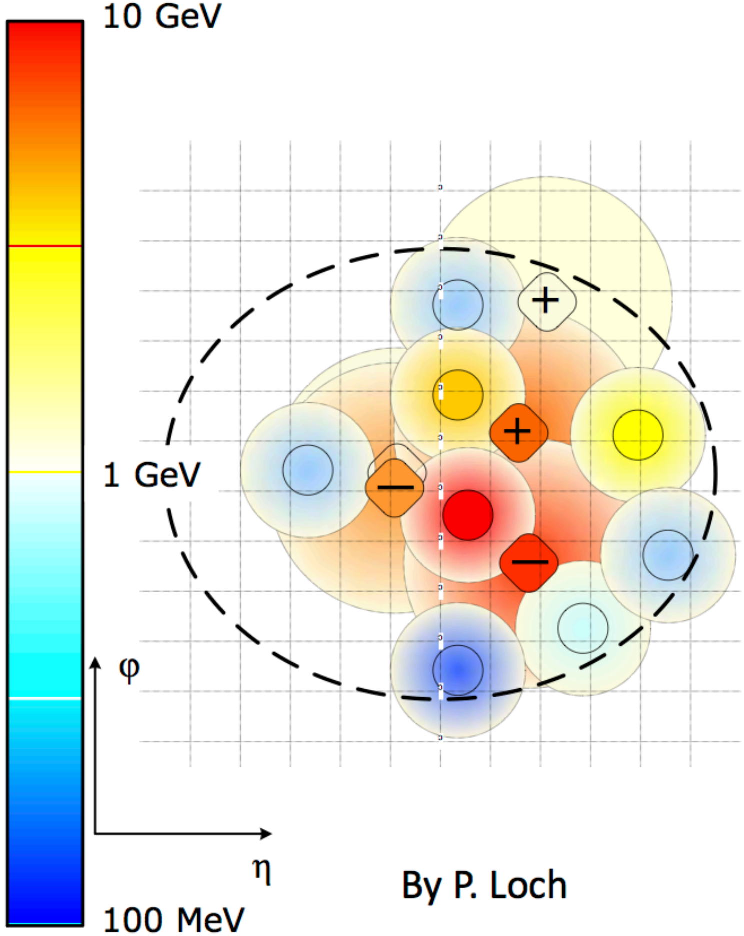

By P. Loch

Change of composition

- Radiation and decay inside detector volume
- "Randomization" of original particle content

Defocusing changes shape in lab frame

- Charged particles bend in solenoid field

Attenuation changes energy

- Total loss of soft charged particles in magnetic field
- Partial and total energy loss of charged and neutral particles in inactive upstream material

Hadronic and electromagnetic cacades in calorimeters

- Distribute energy spatially
- Lateral particle shower overlap

KTH Engineering Sciences

Build Jets from topo-clusters (or towers)

- Different algorithms exists
- Since jets may overlap and be large they must have split/merge criteria

- ATLAS uses anti-k_T with R=0.4 or R=0.6
  (See e.g.: M. Cacciari, G. P. Salam and G. Soyez,
  The anti-k_t clustering algorithm, JHEP 2008 063.)

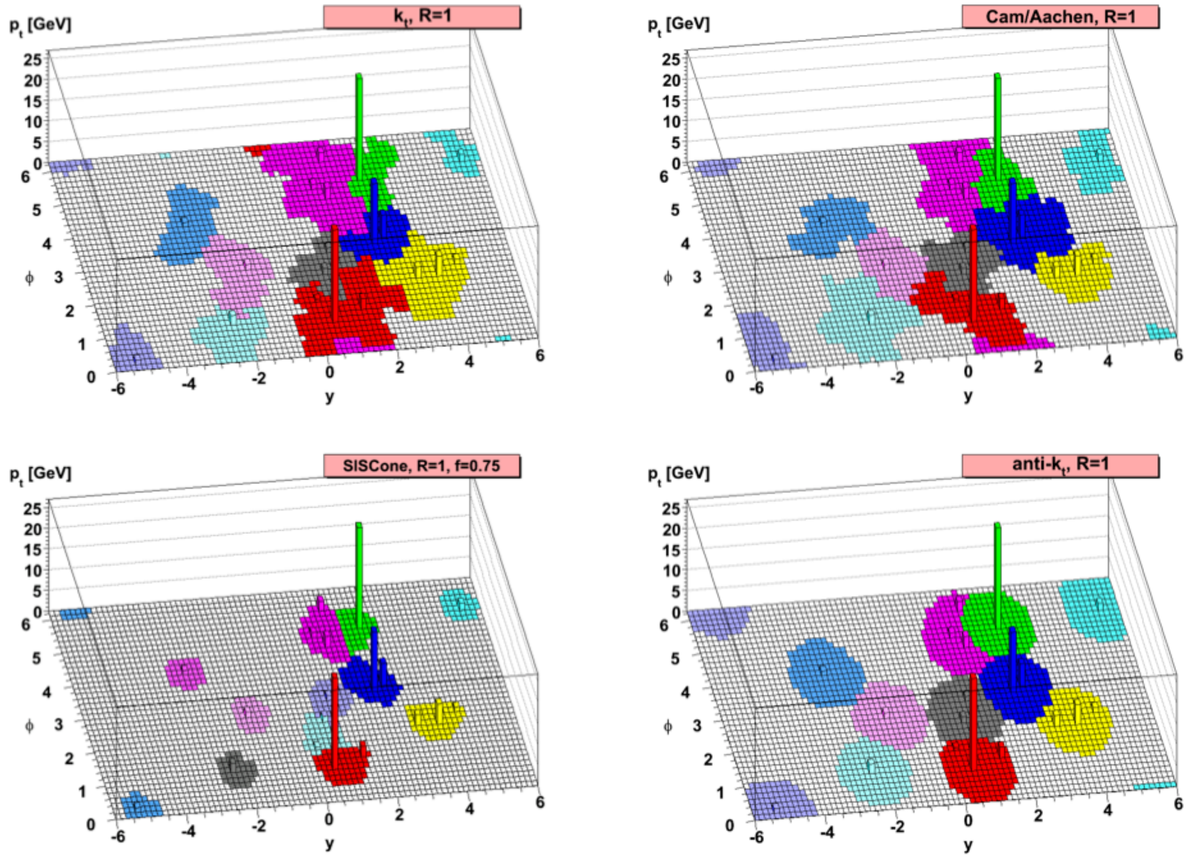

Figure 1: A sample parton-level event (generated with Herwig [8]), together with many random soft "ghosts", clustered with four different jets algorithms, illustrating the "active" catchment areas of the resulting hard jets. For k_t and Cam/Aachen the detailed shapes are in part determined by the specific set of ghosts used, and change when the ghosts are modified.

(From Cacciari, Salam and Soyez)

KTI

Calibration

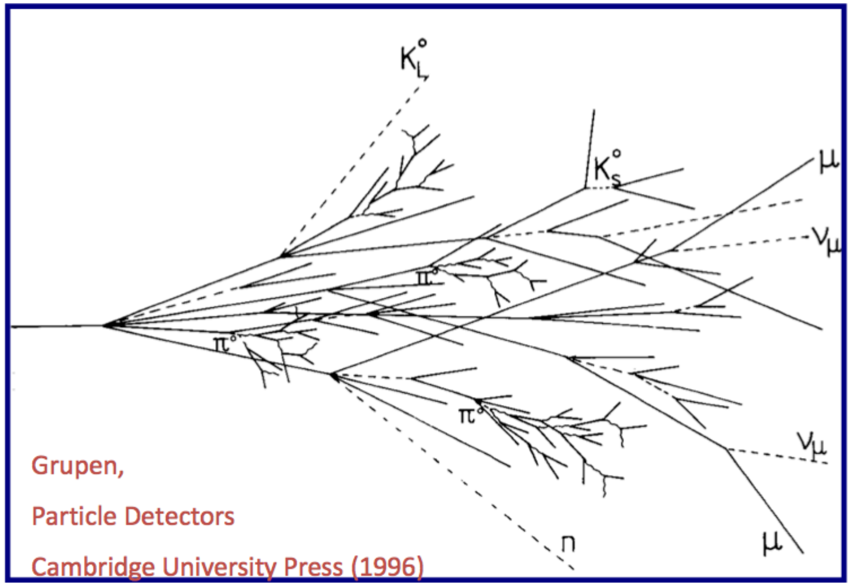

Grupen,
Particle Detectors
Cambridge University Press (1996)

- **Calorimeter non-compensation**
  partial measurement of the energy deposited by hadrons
- **Dead material**
  energy losses in inactive regions of the detector
- **Leakage**
  energy of particles reaching outside the calorimeters
- **Out of calorimeter jet radiation**
  energy deposits of particles inside the truth jet entering the detector that are not included in the reconstructed jet
- **Noise thresholds and particle reconstruction efficiency** signal losses in the calorimeter clustering and jet reconstruction

(M Weber 2012)

KTI

Jet response

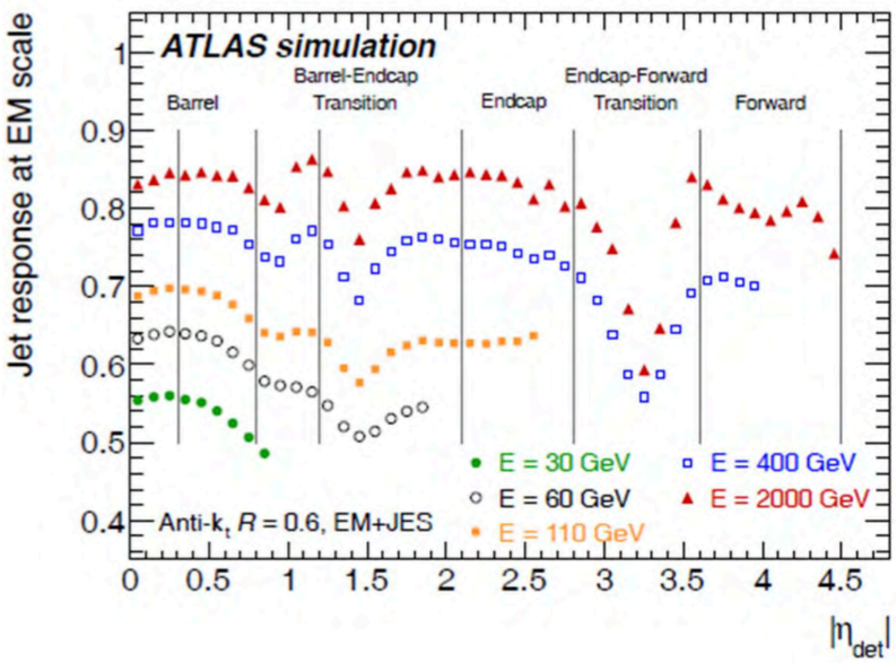

NOT A SMALL CORRECTION...

- Based ok MC (without MPI, as offset already corrected)
- Lines depicts the eta boundaries for the **corrections, which will be averages**

(M Weber 2012)

ATLAS knows several correction 'levels'

- Start from 'EM scale'
  - Apply an absolute calibration derived from test-beam measurements based on EM-showers
    - Test with muons (test-beam, MC, cosmics)
    - Test with Z-> ee
- Apply a 'simple' JES
  - Correct for lower detector response to hadrons
  - Cell based
- More 'realistic' scales
  - Cluster-by-cluster, jet-by-jet
  - Use in-situ calibrations

(M Weber 2012)

optional

data driven

MC

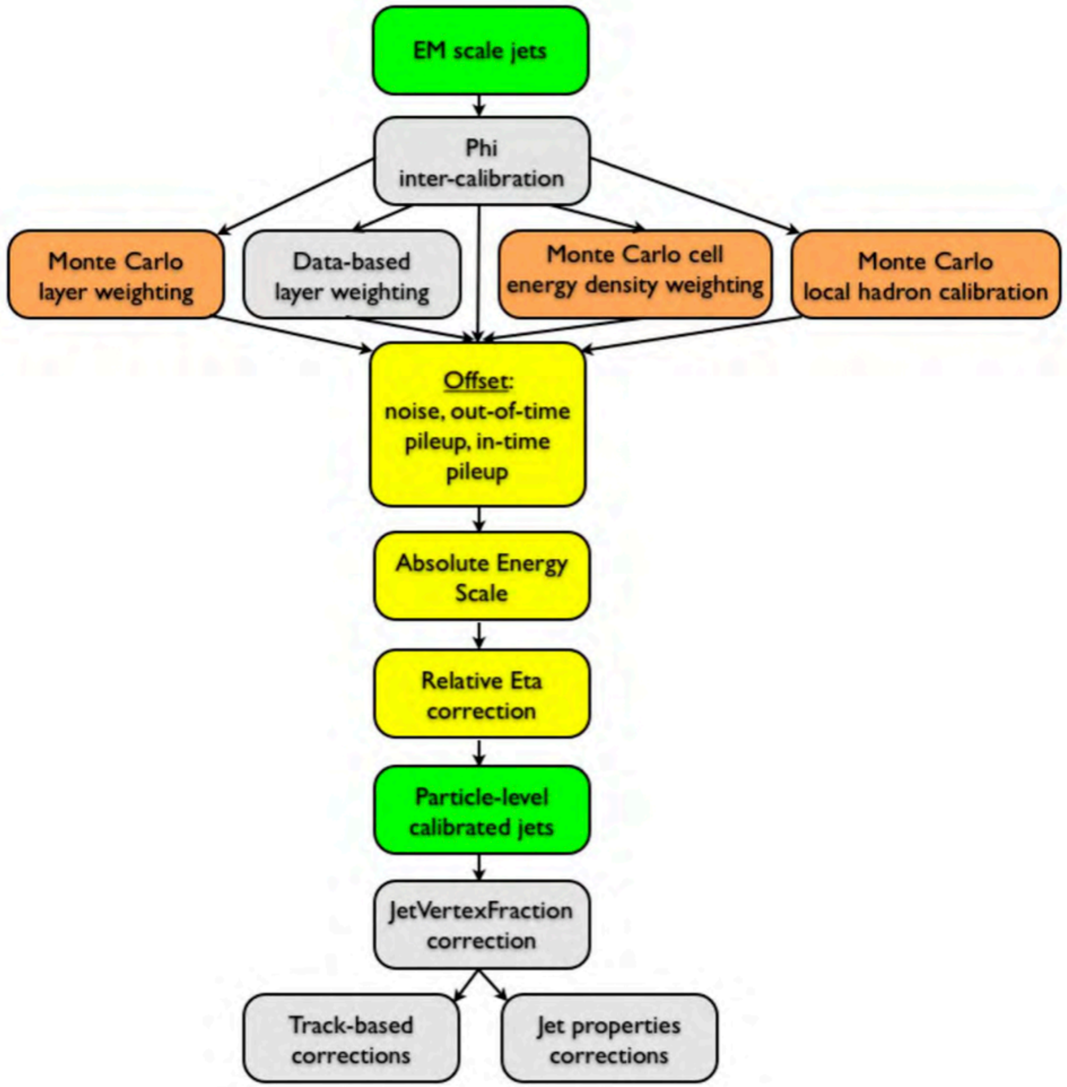

(M Weber 2012)

Other Corrections

- **Pile-up correction**:
  average additional energy due to additional proton-proton interactions (correction from *in situ* measurements)
- **Jet origin correction**:
  Correct the direction of the jet to originate from the primary vertex, no effect on energy
- **Jet energy and direction correction**:
  Correction based on constants derived from the comparison of the kinematic observables of reconstructed jets and those from truth jets (MC).

(M Weber 2012)

Tracking Input to Jet Reconstruction

Program to use tracking information to improve calorimeter jet energy reconstruction and resolution

New approach, conceptually different from energy flow techniques:

Jet energy resolution of non-compensating calorimeters is driven by the jet-to-jet fluctuations in the EM content of the hadronic shower:

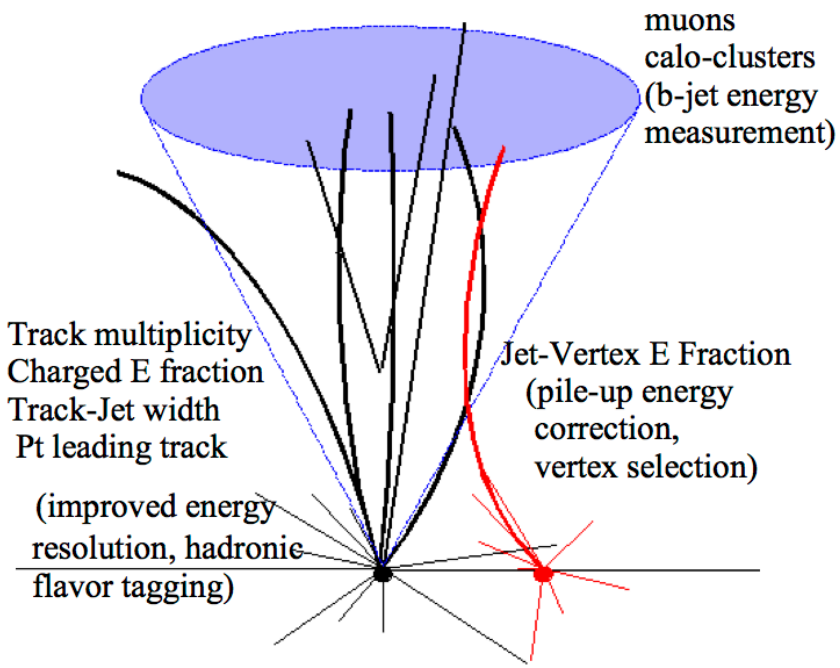

Use tracks to extract information about jet topology and fragmentation, and correct jet response as a function of (track) jet particle composition

(Ariel Schwartzman SLAC)

Jet substructure

At LHC energies

- Heavy new particles e.g. Z' may appear
  Their decay products, although massive, may be Lorentz boosted
- For other reasons massive particles, e.g. Z, W, top may be boosted
- Jets from hadronic decays of boosted particles will be collimated and may appear as one
- We have multiple proton-proton interactions per bunch crossing

For these reasons techniques to disentangle subjets or to “prune” less relevant energy are required.

KTH Engineering Sciences

Mass drop splitting and filtering

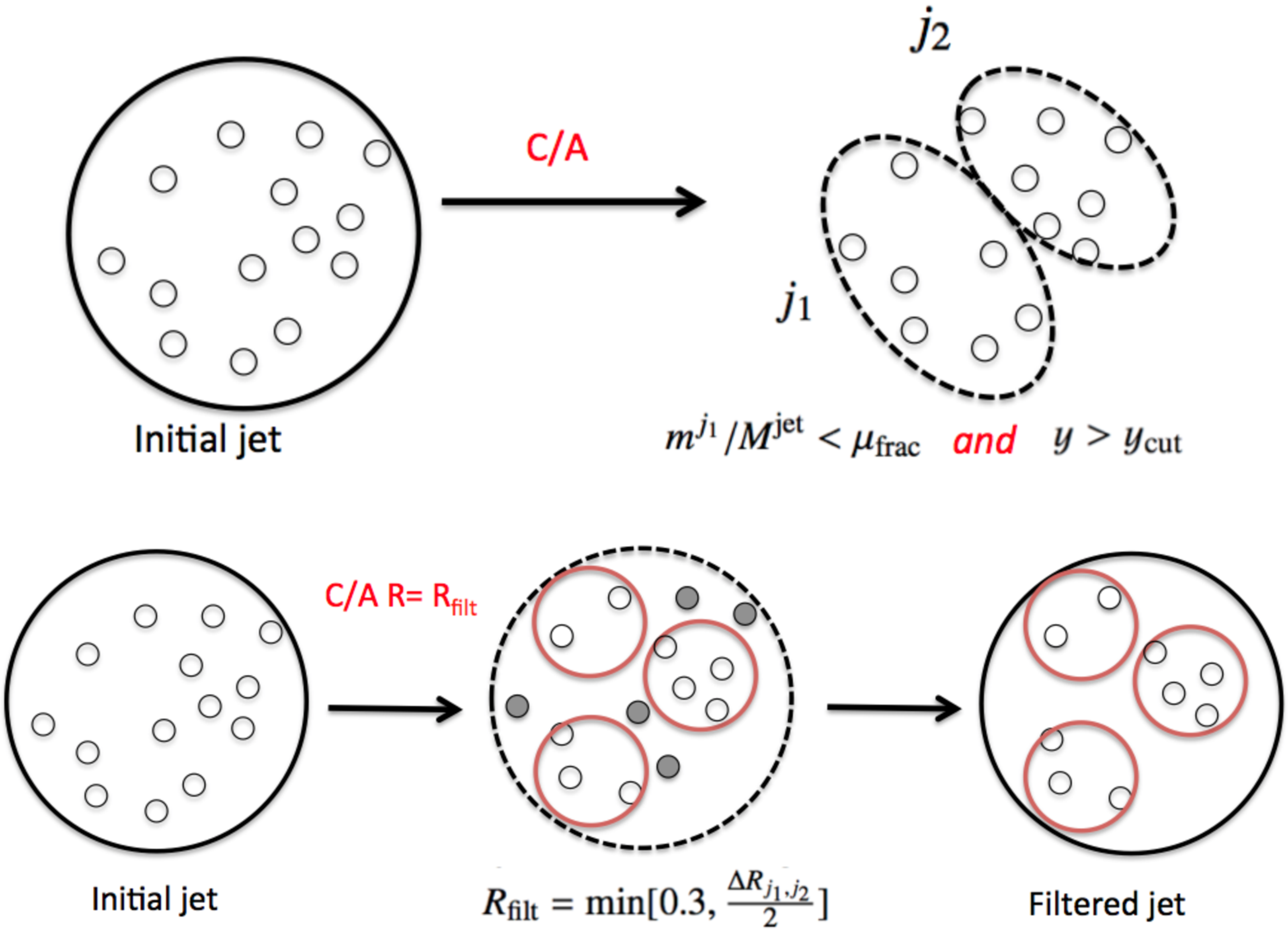

Jet triming

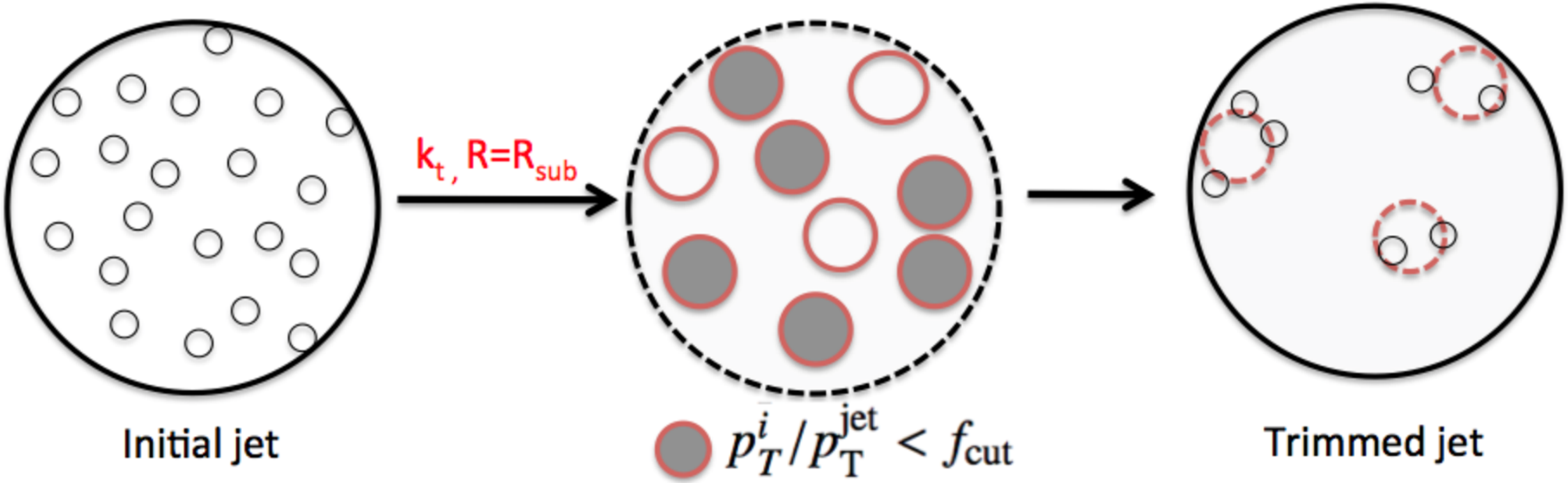

Jet pruning

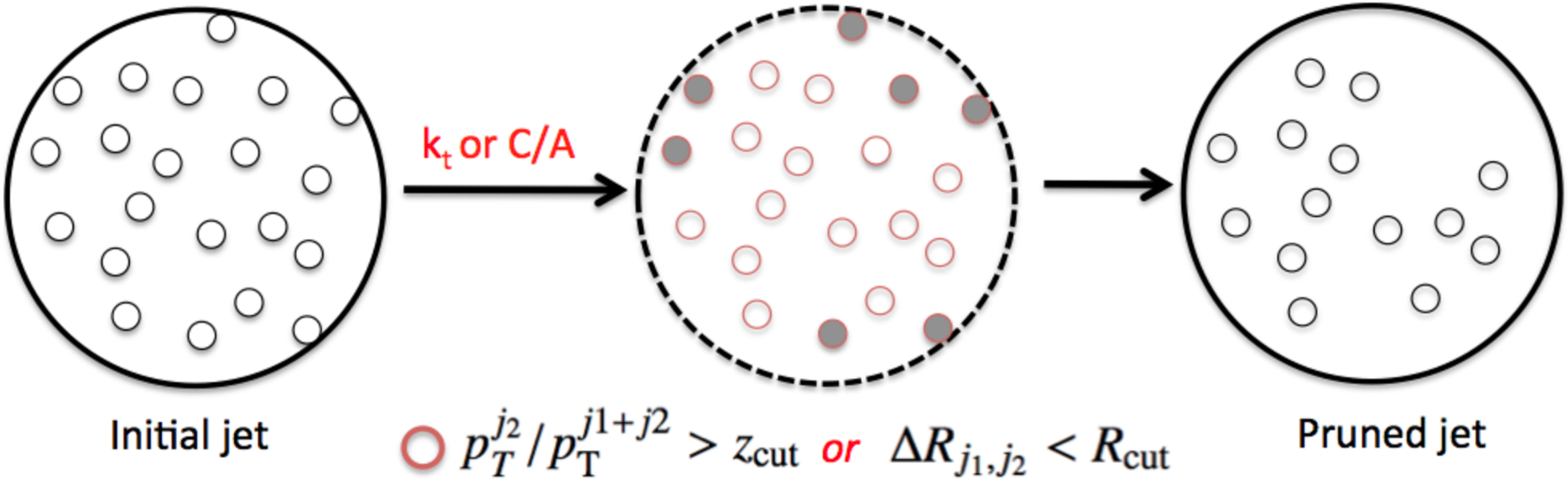
k_t or C/A
Initial jet
$p_T^{j2} / p_T^{j1+j2} > z_{cut}$ or $\Delta R_{j_1,j_2} < R_{cut}$
Pruned jet

❶ Particle Flow Calorimetry

★ **In a typical jet :**

- 60 % of jet energy in charged hadrons
- 30 % in photons (mainly from $\pi^0 \to \gamma\gamma$)
- 10 % in neutral hadrons (mainly n and K_L)

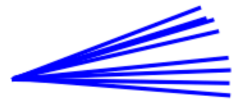

★ **Traditional calorimetric approach:**

- Measure all components of jet energy in ECAL/HCAL !
- ~70 % of energy measured in HCAL: $\sigma_\mathrm{E}/\mathrm{E} \approx 60\,\%/\sqrt{\mathrm{E(GeV)}}$
- Intrinsically "poor" HCAL resolution limits jet energy resolution

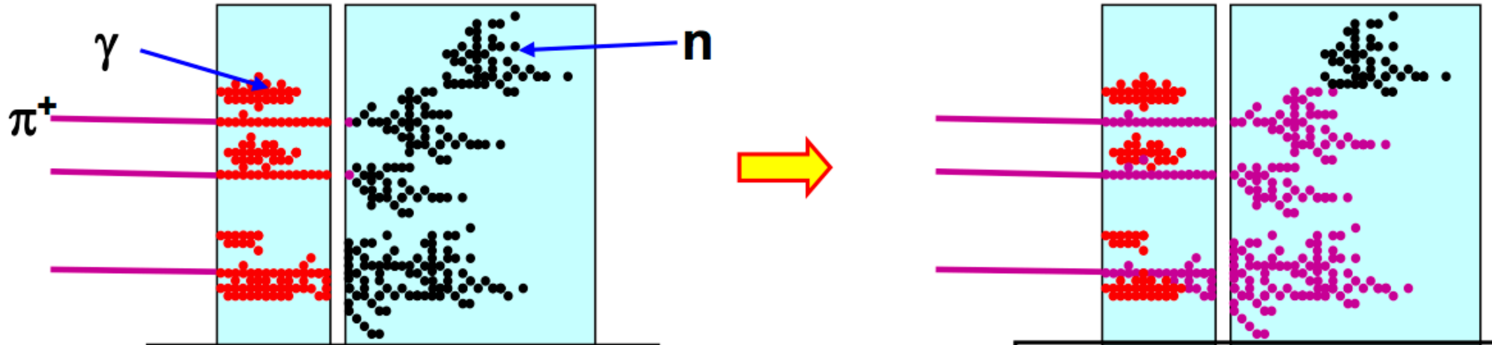

$E_{JET} = E_{ECAL} + E_{HCAL}$

$E_{JET} = E_{TRACK} + E_{\gamma} + E_{n}$

★ **Particle Flow Calorimetry paradigm:**

- charged particles measured in tracker (essentially perfectly)
- Photons in ECAL: $\sigma_\mathrm{E}/\mathrm{E} < 20\,\%/\sqrt{\mathrm{E(GeV)}}$
- Neutral hadrons (ONLY) in HCAL
- Only 10 % of jet energy from HCAL ⟹ much improved resolution

Particle Flow Reconstruction

Reconstruction of a Particle Flow Calorimeter:

- ★ Avoid double counting of energy from same particle
- ★ Separate energy deposits from different particles

e.g.

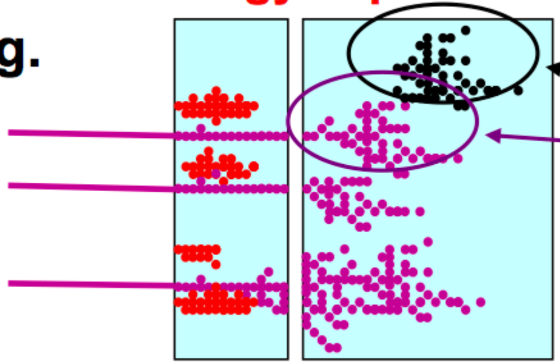

If these hits are clustered together with these, lose energy deposit from this neutral hadron (now part of track particle) and ruin energy measurement for this jet.

Level of mistakes, "confusion", determines jet energy resolution not the intrinsic calorimetric performance of ECAL/HCAL

Three types of confusion:

i) Photons

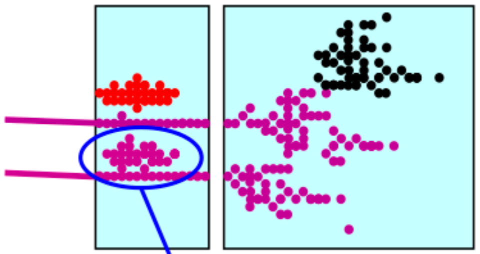

Failure to resolve photon

ii) Neutral Hadrons

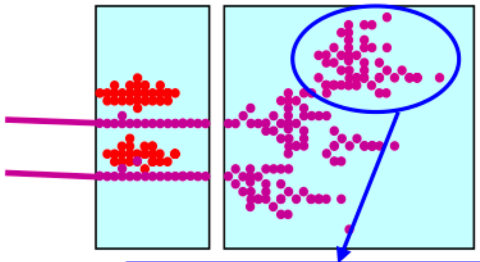

Failure to resolve neutral hadron

iii) Fragments

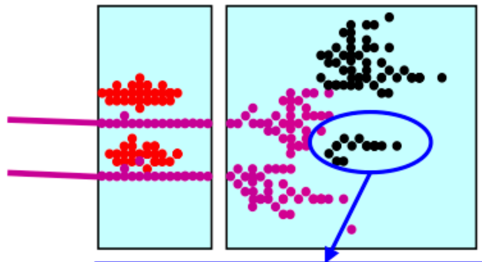

Reconstruct fragment as separate neutral hadron

Particle Flow is not new…

★ First used by ALEPH
★ Major effort in CMS

What's new is…

★ Application to novel high granularity Collider detectors
★ Has driven the design of Linear Collider detectors (ILC and CLIC)

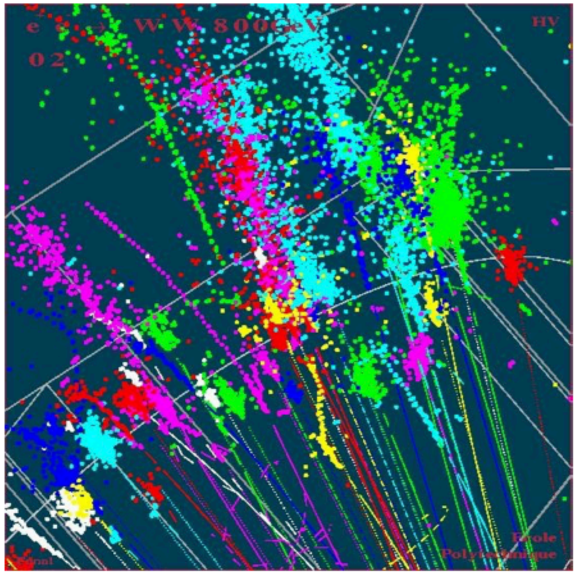

❸ PandoraPFA Algorithm

★**High granularity Pflow reconstruction is highly non-trivial !**

PandoraPFA consists of a many complex steps (not all shown)

❹

Clustering

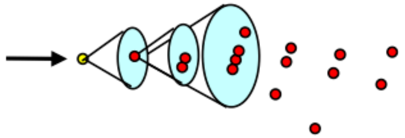

Topological Association

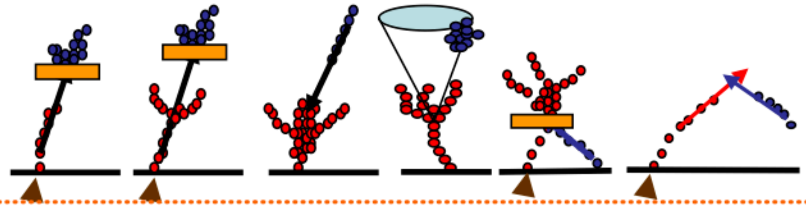

Iterative Reclustering

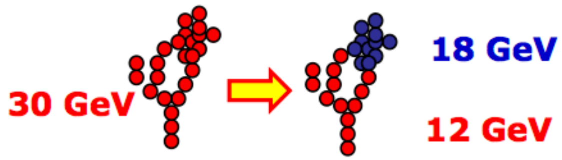

Photon ID

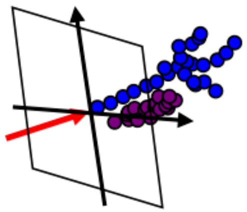

Fragment ID

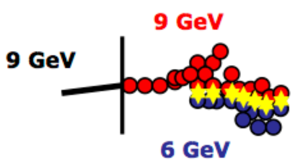

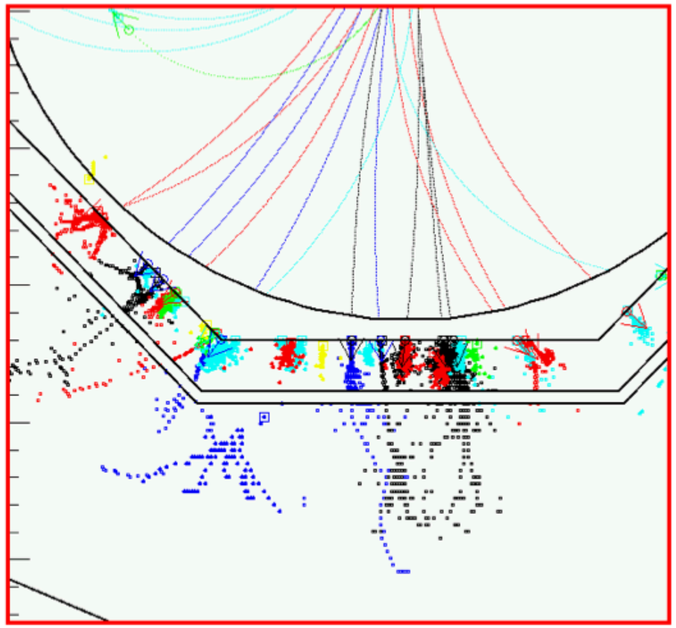

For more details: MT, NIM 611 (2009) 24-40